

**EFFECTS OF GLUCOCORTICOID RECEPTOR BINDING ON BASE
EXCISION REPAIR AT DEOXYURIDINE IN THE GLUCOCORTICOID
RESPONSE ELEMENT**

By

YAN WANG

A thesis submitted in partial fulfillment of
the requirements for the degree of

MASTER OF SCIENCE IN BIOCHEMISTRY

WASHINGTON STATE UNIVERSITY
School of Molecular Biosciences

August 2006

© Copyright by YAN WANG, 2006
All Rights Reserved

To the Faculty of Washington State University:

The members of the Committee appointed to examine the dissertation/thesis of YAN WANG find it satisfactory and recommend that it be accepted.

Chair

ACKNOWLEDGMENT

I would like to thank my advisor, Dr. Michael Smerdon, for his support and guidance throughout my graduate study.

I also want to thank my committee members Dr. Chulhee Kang, Dr. Raymond Reeves, and Dr. John Wyrick for their assistance and the constructive suggestions throughout these years.

Next, I want to thank all the past and present members of the Smerdon lab who have helped me in countless ways over the years: Shubho Chaudhuri, Ronita Nag, Feng Gong, Deirdre Fahy, Shima Nakanishi, Zeljko Svedruzic, Shisheng Li, James Proestos, and Vyacheslav Bespalov.

Finally, I want to thank my mother, to whom I owe too much. Also, I am grateful to my aunt's family for their love and unlimited support throughout these years.

**EFFECTS OF GLUCOCORTICOID RECEPTOR BINDING ON BASE
EXCISION REPAIR AT DEOXYURIDINE IN THE GLUCOCORTICOID
RESPONSE ELEMENT**

Abstract

by Yan Wang, M.S.
Washington State University
August 2006

Chair: Michael J. Smerdon

Glucocorticoid receptor (GR), a ligand-activated transcription factor, has been detected in many different mammalian tissues. In the absence of hormone, GR is sequestered in an inactive form by association in a complex with other proteins. On binding of hormone, the complex is dissociated, leading to release of the active GR which then forms dimers, translocates to the cell nucleus, binds to the glucocorticoid response element (GRE) and triggers transcription activation or repression.

It has been established in previous studies that the presence of DNA binding proteins, such as transcription factor TFIIIA, can modulate repair of lesions in DNA. In this study, we investigated the effect of GR binding on base excision repair (BER) *in vitro*. We initially compared the interaction of the glucocorticoid receptor DNA binding domain (GR-DBD) with intact and uracil-containing GRE DNA. We then examined the efficiency of BER at specific uracil incorporation sites in the GRE following binding of GR-DBD. Recombinant GR-DBD, containing the segment

C440-G525 of the rat glucocorticoid receptor, was expressed and purified to homogeneity. For the binding and repair assays, 80 bp DNA fragments were designed with the GRE sequence in the center. For uracil-containing fragments (dU-GRE), cytosine in the right half site of the GRE was mutated to uracil. The GR-DBD binding affinities of intact and dU-GRE DNA were compared by gel mobility shift assays. As expected, we found that the GR-DBD binding affinity of the dU-GRE fragment was very similar to that of the intact fragment, ~ 0.8 nM. For the repair experiments, we found that access of uracil DNA glycosylase (UDG) and apurinic/apyrimidinic endonuclease (APE) was decreased almost 20-fold following binding of GR-DBD. On the other hand, incorporation of [α - 32 P]dCTP by DNA Polymerase beta (Pol beta) was decreased ~ 2.5 -fold after 4 h incubation following GR-DBD binding, in contrast to the lack of activity we have observed in nucleosome core particles. These results enhance our understanding of the mechanism of DNA damage recognition and repair in protein-DNA complexes.

TABLE OF CONTENTS

	Page
ACKNOWLEDGEMENTS	iii
ABSTRACT	iv
LIST OF TABLES	viii
LIST OF FIGURES	ix
DEDICATION	xi
CHAPTER	
I. INTRODUCTION	1
1. DNA Damage	2
2. DNA Repair Mechanisms	3
2.1. Nucleotide Excision Repair (NER)	4
2.2. Base Excision Repair (BER)	4
2.2.1. Uracil DNA Glycosylase (UDG)	6
2.2.2. Apurinic/Apyrimidinic Endonuclease (APE)	7
2.2.3. DNA Polymerase β (pol β)	9
2.3. Modulation of DNA Repair	9
3. Glucocorticoid (GR) and Glucocorticoid Response Element (GRE)	10
4. Mouse Mammary Tumor Virus Long Terminal Repeat (MMTV-LTR)	12
Figures and Tables	15
References	24

II. PREPARATION OF GR DBD AND DNA SUBSTRATES	28
Summary	29
Materials and Methods.....	30
Results.....	33
Discussion.....	34
Figures and Tables	37
References.....	47
III.EFFECTS OF GLUCOCORTICOID RECEPTOR BINDING ON BASE EXCISION REPAIR OF DEOXYURACIL IN THR GLUCOCORTICOID RESPONSE ELEMENT	48
Summary	49
Introduction.....	50
Materials and Methods.....	53
Results.....	57
Discussion.....	60
Figures and Tables	67
References.....	78

LIST OF TABLES

1. Oligonucleotide Sequences and Abbreviations.....	37
---	----

LIST OF FIGURES

CHAPTER I

1.1. Deamination of Cytosine to Uracil	15
1.2. Base Excision Repair	16
1.3. “Flipped Out” Mechanism of Uracil DNA Glycosylase (UDG)	17
1.4. Glucocorticoid Receptor Signaling.....	18
1.5. Consensus Sequence of GRE.....	19
1.6. Domains of Rat Glucocorticoid Receptor.....	20
1.7. Sequence and Zinc-coordination of the Rat GR DBD (Cys440-Arg510)	21
1.8. Interaction of GR DBD with DNA as a Dimer	22
1.9. Sequential Segment of the Regulatory Region of MMTV-LTR	23

CHAPTER II

2.1. SDS Gel of Cell Lysates before and after IPTG Induction.....	38
2.2. SDS Gel of Ammonium Sulfate Precipitation	39
2.3. Purification on a CM-Sepharose Column	40
2.4. Purification on a Superdex 75 Prep Grade Column.....	42
2.5. Urea Gel of Oligonucleotides before Purification	44
2.6. Gel Extraction and Quantification of Purified DNA	45

CHAPTER III

3.1. MMTV I GRE.....	67
3.2. Comparison of GR DBD Binding to Damaged and Undamaged DNA	68

3.3. Determination of Apparent K _d Values of the GR DBD- DNA Complexes.....	70
3.4. Methylation Protection of Damaged DNA Substrates by GR DBD	72
3.5. UDG/APE Digestions of Free and GR DBD-bound DNA.....	73
3.6. Synthesis by DNA Polymerase β on Free and GR DBD-bound DNA	75
3.7. Hydrogen Bonds between G (-6) and Lys 461.....	77

DEDICATION

This dissertation is dedicated to God my savior, whose power is made perfect in my weakness. To God be glory.

CHAPTER I

INTRODUCTION

DNA damage, DNA repair, GR-GRE complex, and MMTV-LTR

The primary structure of DNA is constantly subjected to damage by a variety of detrimental exogenous and endogenous agents. If DNA damage is not repaired and the cell doesn't undergo apoptosis, it can give rise to mutation fixation, and therefore can lead to cancer or other genetic disorders.

1. DNA Damage

DNA lesions occur from both endogenous and exogenous sources. Within a cell, spontaneous point mutations can occur at high frequency through processes like depurination and deamination. The cytosine to uracil mutation, for instance, has been estimated to occur 100-500 times per day in a human cell (Frederico et al., 1990). Mismatches, small insertions or deletions can be generated during DNA replication. DNA bases can be modified by small molecules involved in metabolism, such as reactive oxygen species (ROS) which are generated as byproducts during normal oxidative metabolism (Madhava and Karen, 2005).

Exogenous sources include UV radiation, ionizing radiation and a host of chemical agents. They can give rise to a variety of DNA lesions like intrastrand crosslinks, interstrand crosslinks, DNA-protein crosslinks, single strand breaks, double strand breaks and base modifications.

The following research focuses on uracil incorporation into DNA, which can arise from spontaneous deamination of cytosine (Figure 1.1), errors in replication, or attacks by small molecules such as bisulfate (Chen and Shaw, 1993) and nitrous acid (Wink et al., 1991). Approximately 200 cytosine deamination events occur each day

in a genome of 10^{10} base pairs, and deamination is expected to occur 1,000 times faster in single-stranded DNA (ssDNA) than in double-stranded DNA (dsDNA), making it a significant event in actively transcribed genes and replication forks (Lindahl, 1979). Additionally, over 10,000 deoxyuridine incorporation events occur per replication cycle in a genome of 10^{10} base pairs (Lindahl, 1979). Misincorporation of uracil produces a G·U base pair which leads to a G·C→A·T transition after a round of DNA replication. This transition can disrupt sequence specific DNA recognition by gene regulatory proteins (Verri et al., 1990), or change the codons of specific genes, all of which will affect normal cell functions (Doetsch, 2002).

2. DNA Repair Mechanisms

As mentioned above, DNA lesions, if not repaired, can cause genomic instability, cancer or cell death. Fortunately, there are a series of repair mechanisms in cells which can remove most of the DNA damage. These include: direct reversal, nucleotide excision repair, base excision repair, mismatch repair and recombinational repair (Sancar et al., 2004). Various repair pathways target different subsets of DNA damage, and deficiencies in any of these pathways can cause increased cancer frequency as well as other abnormalities.

Most types of DNA lesions are repaired by excision repair, which consists of two major pathways: nucleotide excision repair (NER) and base excision repair (BER).

2.1 Nucleotide Excision Repair (NER)

NER is the major repair system for bulky DNA lesions formed by exposure to UV radiation and chemicals, or by crosslinks between protein molecules and DNA. Because of the wide substrate range, excision repair cannot possibly recognize the specific chemical groups that make up the lesion, but is thought to recognize the phosphodiester backbone conformations created by the damage (Sancar et al., 2004). In mammalian cells, about 30 polypeptides are involved in NER. NER can be divided into two pathways: global genomic repair (GGR) and transcription coupled repair (TCR). GGR can take place at any location in the genome, and is initiated by binding of a damage recognition factor. TCR utilizes the blockage of RNA polymerase for damage recognition. The basic steps of NER are (a) damage recognition, (b) dual incisions bracketing the lesion to form a 12-13-nt oligomer in prokaryotes or a 24-32-nt oligomer in eukaryotes, (c) release of the incised oligomer, (d) repair synthesis to fill in the resulting gap and (e) ligation (Friedberg et al., 1995).

2.2 Base Excision Repair (BER)

From its name, we can envision that BER copes with inappropriate bases. These anomalous bases may arise from replication errors, deleterious cellular metabolites or environmental mutagens. In addition, BER is also responsible for the repair of sites of base loss that are formed by enzyme-catalyzed, spontaneous or mutagen-induced base release, and strand breaks that are products of free radical attack of DNA.

Similar to NER, BER involves the concerted effort of several repair proteins that recognize and excise specific DNA lesions, eventually replacing the damaged base moiety with a normal nucleotide and restoring the original DNA sequence (Figure 1.2). However, unlike NER, there is not a common recognition factor in BER. Each type of DNA glycosylase is specific for a specific type of base damage. There are DNA glycosylases that recognize oxidized/reduced bases, alkylated (usually methylated) bases, deaminated bases (e.g., uracil, xanthine), or base mismatches (Sancar et al., 2004). Most DNA glycosylases catalyze only the hydrolytic removal of the target base so as to form an apurinic/apyrimidinic (AP) site, and then the phosphodiester backbone of the AP site is cleaved 5' to the sugar moiety by AP endonuclease. On the other hand, some DNA glycosylases, generally those removing oxidized bases, perform the functions of both the simple glycosylases and the AP endonuclease (Sancar et al., 2004).

After the AP endonuclease reaction, the subsequent steps of BER can be subdivided into two pathways: the long patch pathway (2-10 nucleotide replacement) and DNA polymerase β (pol β)-dependent short-patch pathway (1 nucleotide replacement). For the long patch pathway, the combination of DNA pol δ/ϵ , PCNA, and FEN1 displaces the strand 3' to the nick to produce a flap of 2-10 nucleotides, which is cut at the junction of the single to double strand transition by FEN1 endonuclease. A patch of the same size is then synthesized by pol δ/ϵ with the aid of PCNA, and is ligated by DNA ligase I (Frosina et al., 1996; Klungland and Lindahl, 1997). Previous results show that pol β can also take part in a long patch pathway

(Prasad et al., 2000). For the short patch pathway, subsequent to 5' "nicking" by AP endonuclease, pol β fills in the 1-nucleotide gap, and then the deoxyribose phosphatase (dRP) activity of pol β removes the 5'-dRP moiety (Srivastava et al., 1998). The resulting nick is sealed by the DNA ligase III-XRCC1 complex. The removal of uracil occurs via this pathway.

The discrimination between whether the short patch or the long patch pathway will be utilized is still unclear. Either one of them can be predominant depending on the tissue type (Sancar et al., 2004).

Since the remainder of this thesis will be confined to the short patch BER pathway acting on deoxyuridine (dU), the features of each enzyme involved in this pathway are discussed below:

2.2.1 Uracil DNA Glycosylase (UDG)

UDG is a simple glycosylase which specifically recognizes deoxyuridine in DNA and cleaves the N-glycosidic bond leaving an apyrimidinic site. UDG activity is biologically ubiquitous and highly conserved. For example, UDGs from *E.coli* (Varshney et al., 1988), herpes simplex virus (Savva et al., 1995), *Saccharomyces cerevisiae* (Percival et al., 1989) and humans (Olsen et al., 1989; Mol et al., 1995) have strikingly high similarity in their sequences and structures. In particular, the proteins of human and bacterial origin were unexpectedly found to be most closely related, having about 73.3% similarity (Olsen et al., 1989). UDG is a single domain α/β protein that has a distinctive groove located at the C-terminal edge of a central

four-stranded β sheet which is formed by residues absolutely conserved in all UDGs (Savva et al., 1995; Mol, Arvai, et al., 1995; see Figure 1.2). There are also conserved amino acids within this groove whose side chains prevent binding to RNA and thymines in DNA (Mol, Arvai, et al., 1995).

Study of the crystal structure of human UDG has led to the proposal of a “flipped out” mechanism, or “pinch-push-pull” mechanism (Figure 1.3). It is demonstrated that UDG flips the uracil base and the deoxyribose out of the double helix by compressing the phosphodiester backbone $\sim 20^\circ$ at the deoxyuridine nucleotide and inserting the side chain of a conserved leucine into the minor groove. Thus, the base is pushed into the active-site groove where catalytically important interactions can occur (Slupphaug et al., 1996; Parikh et al., 1998; Mol, Arvai, et al., 1995). Hence it is reasonable that UDG removes uracil from ssDNA three times faster than from dsDNA (Panayotou et al., 1998), since in ssDNA no base flipping is required. Using the proposed “flipped out” mechanism, it also can be explained that the binding of UDG to a G·U mismatch is significantly stronger than to an A·U base pair (Panayotou et al., 1998), since the G·U base pair is less stable than the A·U base pair and uracil in the G·U base pair can be flipped out more easily.

2.2.2 Apurinic/Apyrimidinic Endonuclease (APE)

After the damage-recognition step of BER by UDG or other specific DNA glycosylases, an abasic site (AP site) is generated. Abasic sites can also be created directly in DNA by spontaneous depurination and depyrimidination (Loeb and Preston,

1986), as well as by direct attack of oxygen radicals (Loeb and Preston, 1986; Von Sonntag, 1987). AP sites are a common intermediate in BER. The AP sites, if not repaired, can cause mutagenesis (Zhou and Doetsch, 1993) and apoptosis (Pourquier et al., 1997).

APEs specifically recognize AP sites in double-stranded DNA, and cleave the DNA phosphodiester backbone at a position 5' to AP sites, creating a deoxyribose 5'-phosphate and a 3'-hydroxyl nucleotide. Divalent metal ions are required for this function. Approximately, there are ~ 350,000 to 700,000 APE molecules in a human cell (Chen et al., 1991).

In humans, AP sites are processed by APE1 (also called HAP1, REF1, or APEX), which is homologous to the *E.coli* enzyme Exonuclease III (Exo III). Structures of both reveal the characteristic four-layered α,β -sandwich fold (Mol, Kuo, et al., 1995; Gorman et al., 1997; see Figure 1.2). They share a conserved Asp-His pair that deprotonates a water molecule for nucleophilic attack on the DNA phosphate 5' of the abasic site.

Unlike the induced-fit conformational change in UDG, triggered by base flipping, APE electrostatically orients a rigid, pre-formed DNA-binding face and penetrates the DNA helix from the major and minor grooves on one side of the helix. This stabilizes an extrahelical conformation for abasic nucleotides and excludes normal DNA nucleotides (Mol, Izumi, et al., 2000). Binding of APE introduces a bend of $\sim 35^\circ$ to DNA (Mol, Hosfield, et al., 2000).

2.2.3 DNA Polymerase β (pol β)

Mammalian pol β s are highly conserved at the primary and secondary structure levels (Wilson, 1990). Pol β is a 39 KDa single chain polypeptide comprising 335 amino acid residues (see Figure 1.2). The \sim 8 KDa amino-terminus recognizes and binds to the 5'-phosphate in gapped ssDNA (Kumar, Widen, et al., 1990). It catalyzes the 2'-deoxyribose-5'-phosphate (dRP) lyase reaction that removes the 5'-deoxyribose phosphate after incision by the AP endonuclease (Matsumoto and Kim, 1995). The \sim 31 KDa carboxy-terminal domain is responsible for the nucleotidyl transferase activity (Kumar, Abbotts, et al., 1990), and also exhibits weak double-stranded DNA binding affinity (Casas-Finet et al., 1992). The crystal structure has revealed that pol β binds nicked DNA with a 90° kink in the template strand occurring precisely at the 5'-phosphodiester linkage of the template residue. This allows the 8 KDa lyase domain to access the downstream oligomer 5'-end in the nicked DNA substrate (Sawaya et al., 1997).

2.3 Modulation of DNA repair

DNA repair can be affected by both binding of transcription factors and binding of histone octamers. Slow repair of promoter regions caused by binding of transcription factors has been observed both *in vivo* (Gau et al., 1994; Tu et al., 1996; Tommasi et al., 2000) and *in vitro* (Conconi et al., 1999). The relationship between NER and binding of a transcription factor, TFIIA, has been well studied in the Smerdon lab. Former work has shown that binding of TFIIA to the 5S rRNA gene

can be affected by a single cyclobutane thymine dimer (CTD) in the internal control region (ICR) where TFIIA binds (Kwon and Smerdon, 2003). Furthermore, binding of TFIIA to the 5S rRNA gene can also decrease the rate of NER of CTDs in the ICR (Conconi et al., 1999).

As for BER, Beard et al. (2003) demonstrated that UDG and APE carry out their combined catalytic activities with reduced efficiency on nucleosome substrates containing a dU mutation. Furthermore, they showed that synthesis of pol β is completely inhibited by nucleosome substrates. Nilsen et al. (2002) also investigated BER in nucleosome core particles utilizing the 5S rRNA gene containing a single dU. These authors found that the two limiting steps for repair of nucleosome core particles are the initial excision of uracil and the activity of pol β .

All the former work mentioned above prompted us to examine effects of binding of transcription factors on BER. In the present study, how binding of the glucocorticoid receptor would affect BER in its recognition sequence, the glucocorticoid response element, was examined.

3. Glucocorticoid Receptor (GR) and the Glucocorticoid Response Element (GRE)

GR, a ligand-activated transcription factor, has been detected in many different mammalian tissues. It is almost unique in the receptor family in its restriction to the cytoplasm of a cell in the absence of ligand (Htun et al., 1996). In the absence of hormone, GR is sequestered in an inactive form by association in a complex with

other proteins. Upon binding of hormone, the complex is dissociated, leading to release of the active GR which then forms dimers, translocates to the nucleus, binds to GREs and triggers transcription activation or repression. Dimer formation may occur either prior to, or concurrent with, translocation to the nucleus and binding to specific GREs in the vicinity of regulated genes (Tsai et al., 1988; Wrangé et al., 1989; Cairns et al., 1991) (Figure 1.4).

The 15 bp GRE can be a perfect or imperfect palindrome which has two inverted repeat sequences separated by three nucleotides. The right half-site of GRE is always TGTTCT, but the left half-site can differ (Figure 1.5). The differences in sequences can cause differences in their ability to function as response elements (Ham et al., 1988).

GR has a M_r between 85,000 and 95,000 (Rousseau, 1984). As a member of the steroid receptor family, GR consists of three structural domains: the N-terminal domain, the DNA-binding domain and the C-terminal domain (Kumar and Thompson, 1999) (Figure 1.6). The N-terminal domain of GR is required for full transcriptional activity and it is the most variable in size and amino acid composition. The DNA-binding domain, which is the most conserved among the members of the steroid-thyroid-retinoid super family, contains two zinc fingers formed by the tetrahedral co-ordination of two zinc atoms by four pairs of cysteines (Figure 1.7). The tertiary structure of GR DBD contains three α -helices. Helices I and III are oriented perpendicular to each other. Helix I interacts with the major groove of DNA and is responsible for site-specific discrimination of binding. Helix III is responsible

for less specific DNA interactions. Helix II is formed during DNA binding and its function is not clear (Kumar and Thompson, 1999) (Figure 1.8). The C-terminal domain is required to form the hormone-binding site. It also contains regions required for binding to other receptor-associated proteins, and regions responsible for dimerization and activation of transcription (Kumar and Thompson, 1999).

There are two segments within GR mainly responsible for dimerization. One resides in the C-terminal domain as mentioned earlier; the other is a five amino acid segment at the base of the second zinc finger known as the D-box (residues 458-462; Figure 1.6) (Dahlman-Wright et al., 1991).

There are also two regions in GR responsible for nuclear localization. One is a region enriched in basic amino acids immediately adjacent to the second zinc finger; the other is present in the hormone-binding domain of the GR and it is functional upon hormone binding (Picard and Yamamoto, 1987).

4. Mouse Mammary Tumor Virus Long Terminal Repeat (MMTV-LTR)

The MMTV-LTR has served as the prototype for studies developing the conceptual framework of the molecular mechanisms of glucocorticoid hormone action, and it is also a useful model for studies on the relationship between chromatin structure and transcriptional activation. In chromosomes, the MMTV-LTR is organized in an array of six nucleosomes, termed A through F. Four receptor binding sites are associated with nucleosome B (-70 to -190) (Richard-Foy and Hager, 1987). Distinct GREs have different contributions to overall transcription stimulation (Figure

1.9). Linker scanning mutagenesis has revealed that mutants in the distal segment (-171 to -185; Figure 1.9) have a reduction of up to 20-fold in the hormone response as compared to wild type. Mutations in the proximal element around position -120 cause a 5-fold reduction. The other two proximal half GREs, although having weak interactions with GR detected *in vitro*, appear to be insufficient for a detectable alteration of the hormone response in the presence of other control elements in a functional assay (Buetti and Kühnel, 1986). Both *in vivo* (McNally et al., 2000) and *in vitro* (Fletcher et al., 2000) research on GR action has suggested a “hit-and run” model in which GR first binds to chromatin after ligand activation, recruits a remodeling activity, and is then lost from the template.

In our study, an 80 bp DNA segment of the MMTV-LTR containing the distal full-length GRE (MMTV I GRE; Figure 1.9) was used as the undamaged DNA substrate. The MMTV I GRE offers the greatest contribution to the overall transcriptional activation; therefore, study of this GRE may provide more clues to the overall function of MMTV-LTR than the other GREs.

In this thesis, the effect of deoxycytidine to deoxyuridine mutation in the MMTV I GRE on GR binding and the effect of GR binding on repair efficiency of this mutation have been examined in naked DNA. Future work on this system should begin to determine the effect of such a mutation on GR binding and effect of GR binding on repair in a nucleosome. The mutation may affect binding of GR, and thus affect the transcriptional activation by this hormone receptor. Furthermore, binding of GR may either recruit chromatin remodeling factors which in turn may facilitate the

repair of DNA lesions in the GRE, or 'shield' DNA lesions from efficient repair.

FIGURES AND TABLES

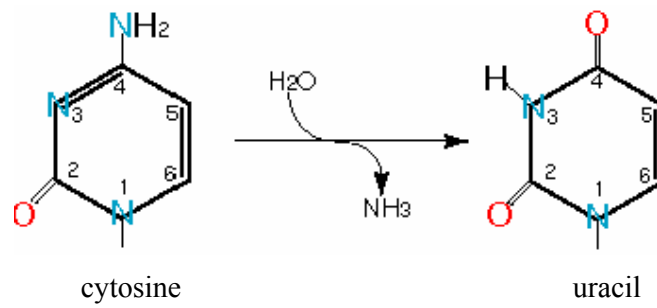


Figure 1.1 Deamination of Cytosine to Uracil. The primary amino group of cytosine is unstable and can be converted to a keto group in a deamination reaction.

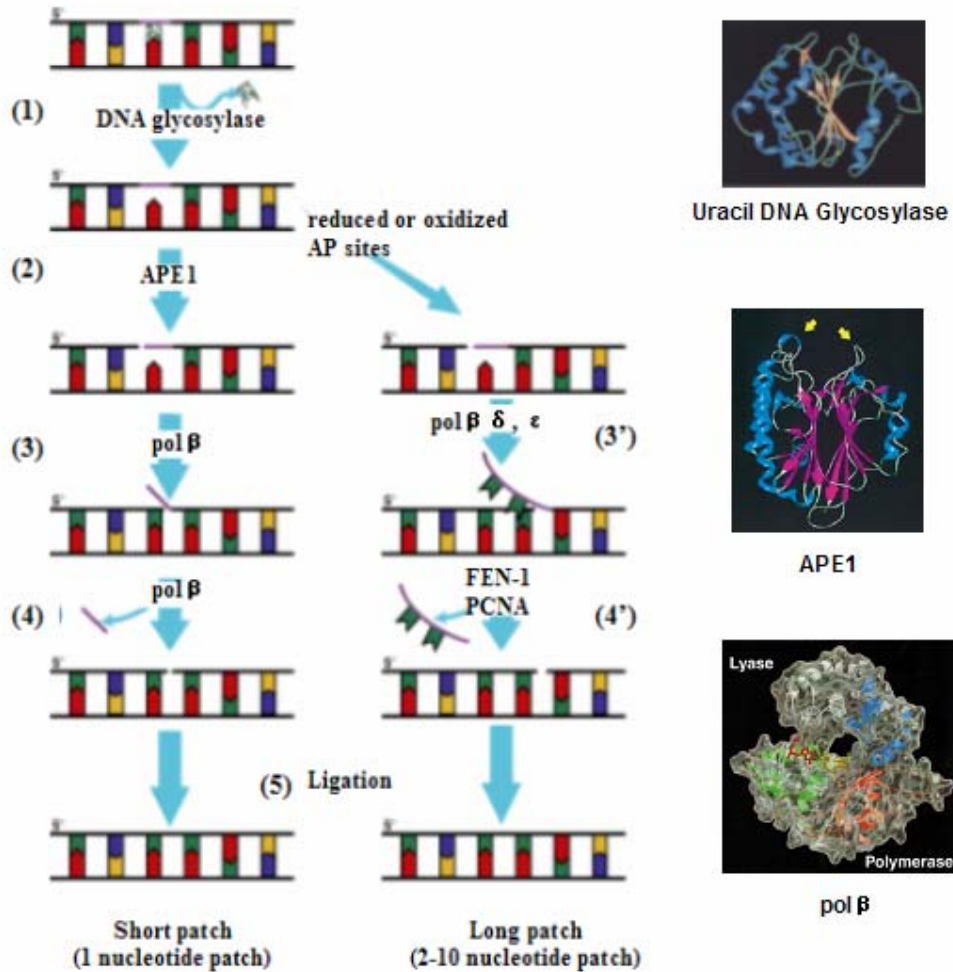


Figure 1.2 Base Excision Repair. Shown is a general model of the short-patch (left) and long-patch (right) BER pathways. (1): DNA glycosylase incision of damaged base [structure from (Mol et al., 1995)]. (2): AP endonuclease cleavage 5' to the AP site [structure from (Gorman et al., 1997)]. (3): DNA polymerase activity of polymerase β [structure from (Beard and Wilson, 2000)]. (3'): DNA synthesis by DNA polymerase δ and ε. (4): Deoxyribosephosphodiesterase activity of DNA polymerase β. (4'): Cleavage of flap by FEN1 and PCNA. (5): Ligation of ssDNA nick by DNA ligase [adapted from: http://www.rndsystems.com/mini_review_detail_objectname_MR03_DNADamageResponse.aspx]. Structures of uracil DNA glycosylase, APE1, and pol β are shown on the right.

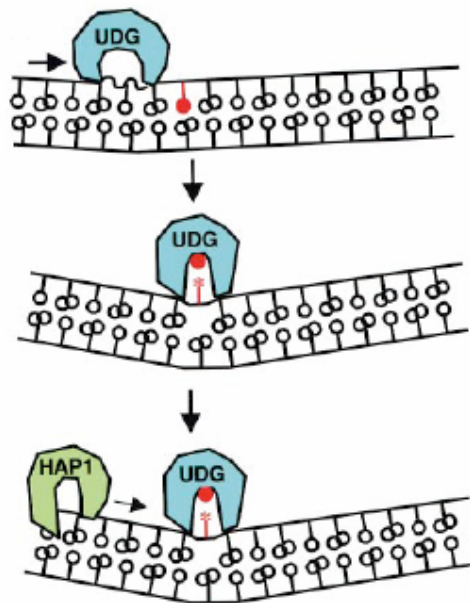


Figure 1.3 “Flipped Out” Mechanism of Uracil DNA Glycosylase (UDG). UDG scans the DNA minor groove for a uracil lesion (red) by compressing the intrastrand DNA backbone and slightly bending the DNA. The uracil-containing nucleotide is detected and flipped out of the DNA base stack and into the UDG active site, causing pronounced DNA bending ($\sim 20^\circ$) and coalescence of the enzyme around the extrahelical uracil and deoxyribose. The glycosylic bond is cleaved, but UDG remains bound to the resultant products, waiting for replacement by human apurimidinic/apurinic endonuclease 1 (HAP1), to avoid the exposure of the cytotoxic AP site. [Adapted from (Parikh et al., 1998)]

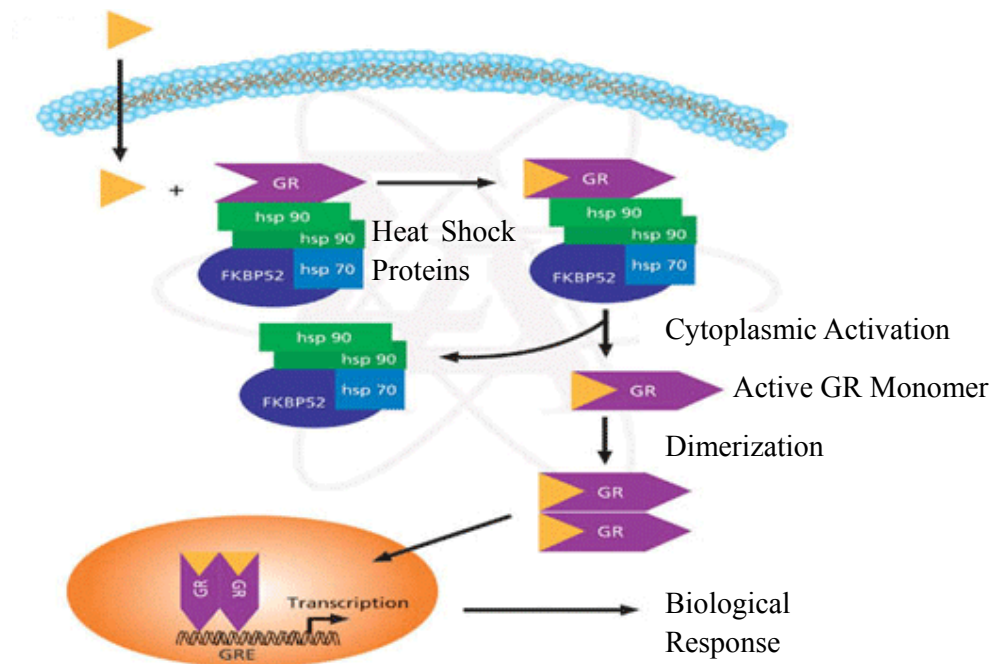


Figure 1.4 Glucocorticoid Receptor Signaling. The glucocorticoid hormone (denoted by a solid triangle) passes through the plasma membrane into the cytoplasm where it binds to the specific, high-affinity GR. The resulting complex is the non-DNA-binding oligomer of the GR, in which the receptor is complexed with other proteins. In this complex, the DNA-binding domain of the receptor is bound by the heat shock protein 90 (hsp90) dimer. Other proteins in this complex include heat shock protein 70 (hsp70) and FKBP52. Dissociation of the oligomeric complex yields the free hormone-receptor subunit in the DNA-binding form. The activated receptor forms a homodimer and is translocated to the nucleus through a nucleopore. Inside the nucleus, the receptor complex binds to specific DNA responsive elements (GREs) to modulate gene transcription [taken from: http://www.sigmaaldrich.com/Area_of_Interest/Life_Science/Cell_Signaling/Scientific_Resources/Pathway_Slides___Charts/Glucocorticoid_Receptor_Signaling.html].



Figure 1.5 Consensus Sequence of GRE. The consensus sequence is derived from all functionally characterized GREs (Jantzen et al., 1987). The 15bp GRE can be a perfect or imperfect palindrome which has two inverted repeat sequences separated by three nucleotides (N represents any nucleotide). Common to all known GREs is the hexanucleotide TGTTCT in the right half-sites. The left half-sites vary in different GREs. The differences in sequences can cause differences in their ability to function as a response element.

Rat glucocorticoid receptor: 795 amino acids

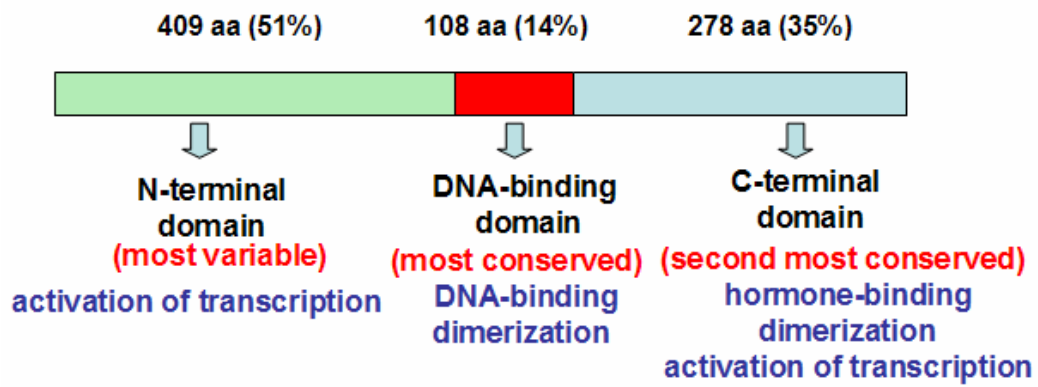


Figure 1.6 Domains of Rat Glucocorticoid Receptor. The functions of each domain are listed in the figure.

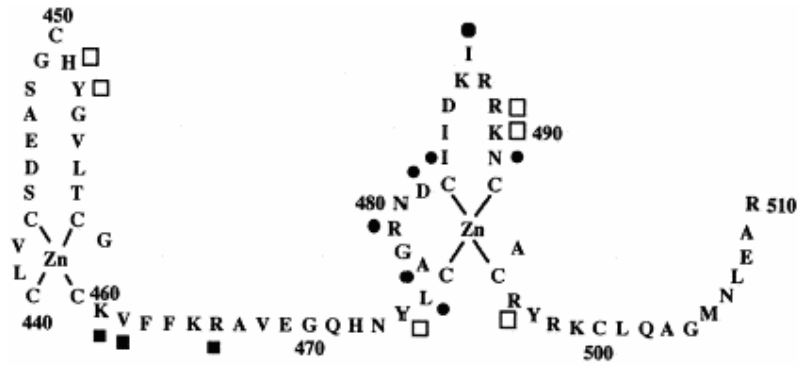


Figure 1.7 Sequence and Zinc-coordination of the Rat GR DBD (Cys440-Arg510). Residues which interact with DNA bases (filled squares) and the phosphate backbone (open squares), and which form the dimer interface (filled circles) are indicated [structure from (Van Tilborg et al., 2000)].

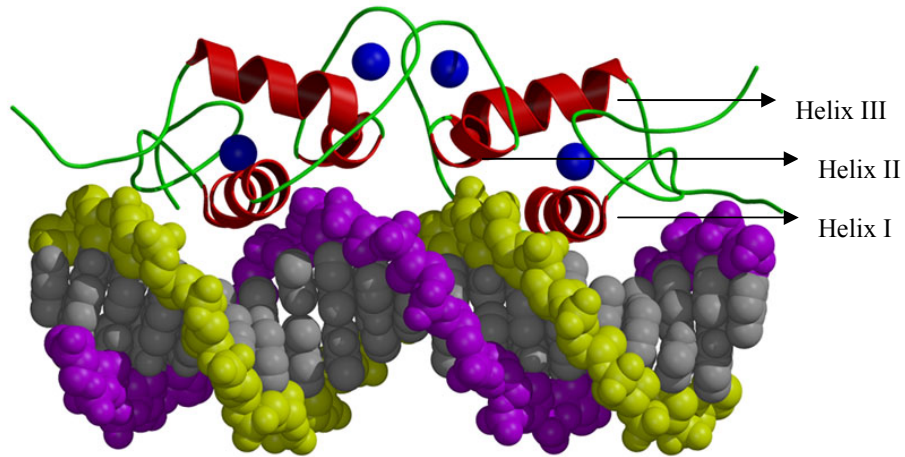


Figure 1.8 Interaction of GR DBD with DNA as A Dimer. GR DBD binds to one face of DNA as a dimer. The tertiary structure of GR DBD contains three α -helices. Helices I and III are oriented perpendicular to each other. Helix I interacts with the major groove of DNA and is responsible for site-specific discrimination of binding. Helix III is responsible for less specific DNA interactions. Helix II is formed during DNA binding and its function is not clear (Kumar and Thompson, 1999) [Modified from the original figure by Dr. Miesfeld, R.L.].

```

      -180           -170           -160           -150
      |             |             |             |
GTTACAAACTTGTTCTTAAAACGAGGATGTGAGACAAG
      |             |             |
      -140           -130           -120
      |             |             |
TGGTTTCCTGACTTGGTTTGGTATCAAATTGTTCTGATC
      |             |             |             |
      -110           -100           -90           -80
      |             |             |             |
TGAGCTCTTAGTTGTTCTATTTTCCATTGTTCTTTTGG

```

Figure 1.9 Sequential Segment of the Regulatory Region of MMTV-LTR. Shown in the figure is the coding strand. It is numbered with respect to the transcription start site. The consensus hexanucleotides are underlined [adapted from (Buetti and Kühnel, 1986)].

REFERENCES

- Baer, R., Bankier, A.T., Biggin, M.D., Deininger, P.L., Farrell, P.J., Gibson, T.J., Hatfull, G., Hudson, G.S., Satchwell, S.C., Seguin, C., et al. (1984) *Nature* Jul 19-25; 310(5974), 207-211.
- Beard, B.C., Wilson, S.H., and Smerdon, M.J. (2003) *Proc Natl Acad Sci U S A.* Jun 24; 100(13), 7465-7470.
- Beard, W.A. and Wilson, S.H. (2000) *Mutat. Res.* 460,231-244.
- Buetti, E. and Kühnel, B. (1986) *J. Mol. Biol.* 190, 379-389.
- Cairns, W., Cairns, C., Pongratz, I., Poellinger, L., and Okret, S. (1991) *J. Biol. Chem.* 266, 11221-11226.
- Casas-Finet, J.R., Kumar, A., Karpel, R.L., and Wilson, S.H. (1992) *Biochemistry* Oct 27; 31(42), 10272-10280.
- Chen, D.S., Herman, V., and Demple, B. (1991) *Nucleic Acids Res.* 19, 5907-5914.
- Chen, H. and Shaw, B.R. (1993) *Biochemistry* 32 (14), 3535-3539.
- Conconi, A., Liu, X., Koriazova, L., Ackerman, E.J., and Smerdon, M.J. (1999) *EMBO J.* Mar 1; 18(5), 1387-1396.
- Dahlman-Wright, K., Wright, A., Gustafsson, J.-A., and Carlstedt-Duke, J. (1991) *J. Biol. Chem.* 266, 3107-3112.
- Doetsch, P.W. (2002) *Mutation Research* 510, 131-140.
- Fletcher, T.M., Ryu, B., Baumann, C.T., Warren, B.S., Fragoso, G., John, S., and Hager, G.L. (2000) *Molecular and Cellular Biology* Sept; 6466-6475.
- Frederico, L.A., Kunkel, T.A., and Shaw, B.R. (1990) *Biochemistry* 29, 2532-2537.
- Friedberg, E. C., Walker, G. C., and Siede, W., (1995) *DNA repair and mutagenesis*, *Am. Soc. Microbiol. Press, Washington DC*.
- Frosina, G., Fortini, P., Rossi, O., Carrozzino, F., Raspaglio, G., et al., (1996) *J. Biol. Chem.* 271, 9573-9578.
- Gau, S., Drouin, R., and Holmquist, G.P. (1994) *Science* 253, 1438-1440.

- Gorman, M.A., Morera, S., Rothwell, D.G., de La Fortelle, E., Mol, C.D., Tainer, J.A., Hickson, I.D., and Freemont, P.S. (1997) *EMBO J.* Nov 3; 16(21), 6548-6558.
- Ham, J., et al. (1988) *Nucleic Acids Res.* 16, 5263-5267.
- Htun, H., Barsony, J., Renyi, I., Gould, D. J., and Hager, G. L. (1996) *Proc. Natl. Acad. Sci. USA.* 93, 4845-4850.
- Jantzen, H., Strähle, U., Gloss, B., Stewart, F., Schmid, W., Boshart, M., Miksicek, M., and Schütz, G. (1987) *Cell* Apr 10; 49, 29-38.
- Klungland, A. and Lindahl, T. (1997) *EMBO J.* 16, 3341-3348.
- Kumar, A., Widen, S.G., Williams, K.R., Kedar, P., Karpel, R.L., and Wilson, S.H. (1990) *J Biol Chem.* Feb 5; 265(4), 2124-2131.
- Kumar, A., Abbotts, J., Karawya, EM., and Wilson, S.H. (1990) *Biochemistry* Aug 7; 29(31), 7156-7159.
- Kumar, R. and Thompson, E.B. (1999) *Steroids* 64, 310-319.
- Kwon, Y. and Smerdon, M.J. (2003) *J Biol Chem.* Nov 14; 278(46), 45451-45459.
- Lindahl, T. (1979) *Prog. Nucleic Acid Res. Molec. Biol.* 22, 135-192.
- Loeb, L.A. and Preston, B.D. (1986) *Annu. Rev. Genet.* 20, 201-230.
- Madhava, C.R. and Karen, M.V. (2005) *Radiation Research* 164, 345-356.
- Matsumoto, Y. and Kim, K. (1995) *Science* Aug 4; 269(5224), 699-702.
- McNally, J.G., Müller, W.G., Walker, D., and Hager, G.L. (2000) *Science* 287, 1262-1264.
- Mol, C.D., Arvai, A., Slupphaug, G., Kavli, B., Alseth, I., Krokan, H.E., and Tainer, J.A. (1995) *Cell* Mar 24; 80(6), 869-878.
- Mol, C.D., Kuo, C.F., Thayer, M.M., Cunningham, R.P., and Tainer, J.A. (1995) *Nature* Mar 23; 374(6520), 381-386.
- Mol, C.D., Izumi, T., Mitra, S., and Tainer, J.A. (2000) *Nature* Jan 27; 403(6768), 451-456.
- Mol, C.D., Hosfield, D.J., and Tainer, J.A. (2000) *Mutat Res.* Aug 30; 460(3-4),

211-229.

Nilsen, H., Lindahl, T. and Verreault, A. (2002) *EMBO J.* 21(21), 5943-5952.

Olsen, L.C., Aasland, R., Wittwer, C.U., Krokan, H.E., and Helland, D.E. (1989) *EMBO J.* Oct; 8(10), 3121-3125.

Panayotou, G., Brown, T., Barlow, T., Pearl, L.H., and Savva, R. (1998) *J Biol Chem.* Jan 2; 273(1), 45-50.

Pankiewicz, K.W., Watanabe, K.A., and Stivers, J.T. (1999) *Biochemistry* Jan 19; 38(3), 952-963.

Parikh, S.S., Mol, C.D., Slupphaug, G., Bharati, S., Krokan, H.E., and Tainer, J.A. (1998) *EMBO J.* Sep 1; 17(17), 5214-5226.

Percival, K.J., Klein, M.B., and Burgers, P.M. (1989) *J Biol Chem.* Feb 15; 264(5), 2593-2598.

Picard, D. and Yamamoto, K. R. (1987) *EMBO J.* 6, 3333-3340.

Pourquier, P., Ueng, L.M., Kohlhagen, G., Mazumder, A., Gupta, M., Kohn, K.W., and Pommier, Y. (1997) *J. Biol. Chem.* Mar 21; 272(12), 7792-7796.

Prasad, R., Dianov, G.L., Bohr, V.A., and Wilson, S.H. (2000) *J. Biol. Chem.* 275, 4460-4466.

Richard-Foy, H. and Hager, G.L. (1987) *EMBO J.* 6, 2321-2328.

Rousseau, G.G. (1984) *Molecular and Cellular Endocrinology* 38, 1-11.

Sancar, A., Lindsey-Boltz, L.A., Unsal-Kacmaz, K., and Linn, S. (2004) *Annu Rev Biochem.* 73, 39-85.

Savva, R., McAuley-Hecht, K., Brown, T., and Pearl, L. (1995) *Nature* Feb 9; 373(6514), 487-493.

Sawaya, M.R., Prasad, R., Wilson, S.H., Kraut, J., and Pelletier, H. (1997) *Biochemistry* Sep 16; 36(37), 11205-11215.

Slupphaug, G., Mol, C.D., Kavli, B., Arvai, A.S., Krokan, H.E., and Tainer, J.A. (1996) *Nature* Nov 7; 384(6604), 87-92.

Srivastava, D.K., Vande Berg, B.J., Prasad, R., Molina, J.T., Beard, W.A., Tomkinson,

- A.E., and Wilson, S.H. (1998) *J. Biol. Chem.* 273, 21203-21209.
- Tommasi, S., Oxyzoglou, A.B., and Pfeifer, G.P. (2000) *Nucleic Acids Res.* 28, 3991-3998.
- Tsai, S.Y., Carlstedt-Duke, J., Weigel, N.L., Dahlman, K., Gustafsson, J.-Å., Tsai, M.J., and O'Malley B.W. (1988) *Cell* 55, 361-369.
- Tu, Y., Tornanaletti, S., and Pfeifer, G.P. (1996) *EMBO J.* 15, 675-683.
- Varshney, U., Hutcheon, T., and van de Sande, J.H. (1988) *J Biol Chem.* Jun 5; 263(16), 7776-7784.
- Verri, A., Mazzarello, P., Biamonti, G., Spadari, S., and Focher, F. (1990) *Nucleic Acids Res.* Oct 11; 18(19), 5775-5780.
- Von Sonntag, C. (1987) *The Chemical Basis of Radiation Biology.* London, NY: Taylor & Francis.
- Van Tilborg, M.A., Lefstin, J.A., Kruiskamp, M., Teuben, J., Boelens, R., Yamamoto, K.R., and Kaptein, R. (2000) *J Mol Biol.* Aug 25; 301(4), 947-958.
- Wilson, S.H. (1990) in Strauss, P.R. and Wilson, S.H. (Eds.), *The Eukaryotic Nucleus: Molecular Biochemistry and Macromolecular Assemblies*, The Telford Press/CRC Press, Caldwell, NJ, pp. 199-234.
- Wink, D.A., Kasprzak, K.S., Maragos, C.M., Elespuru, R.K., Misra, M., Dunams, T.M., Cebula, T.A., Koch, W.H., Andrews, A.W., Allen, J.S., and Keefer, L.K. (1991) *Science* 254, 1001-1003.
- Wrange, Ö., Eriksson, P. and Perlmann, T. (1989) *J. Bio. Chem.* 264, 5253-5359.
- Zhou, W. and Doetsch, P.W. (1993) *Proc Natl Acad Sci U S A.* Jul 15; 90(14), 6601-6605.

CHAPTER II

Preparation of GR DBD and DNA substrates

SUMMARY

We have investigated the effect of deoxyuridine (dU) incorporation into a DNA substrate on glucocorticoid receptor (GR) binding and the effect of GR binding on base excision repair (BER) of dU in the glucocorticoid response element (GRE). As mentioned in the introduction, GR, a member of the intracellular nuclear receptor superfamily, has three major functional domains—an N-terminal domain involved in activation of transcription, a central DNA-binding domain, and a C-terminal ligand-binding domain. The DNA-binding domain (DBD) contains all the residues required for the binding of GR to GRE. Therefore, to simplify the purification process, GR DBD was used in these experiments instead of the entire GR. Recombinant rat GR DBD, containing the segment C440-G525 of the rat GR, was overexpressed in *E.coli* and purified to homogeneity by column chromatography. For the binding and repair assays, an 80 bp DNA segment containing the distal GRE of the MMTV-LTR (MMTV I GRE) was used as the intact DNA substrate. For the uracil-containing fragment (dU-GRE), a cytosine in the right half-site of the GRE was mutated to uracil. The oligonucleotides, purified by high-pressure liquid chromatography (HPLC), were labeled on the 5' ends with [γ -³²P]ATP and T4 polynucleotide kinase, and further purified by gel extraction.

MATERIALS AND METHODS

Preparation of recombinant GR DBD.

Recombinant GR DBD, containing the segment C440-G525 of rat glucocorticoid receptor, was overexpressed from the plasmid pGR440 in the *E.coli* strain BL21 [DE]/pLysS using a modification of the method reported by Lundback et al. (1994). Bacteria were grown at 37°C in LB medium, containing 25 µg/ml ampicillin, to a cell density giving $A_{600} = 0.6$. GR DBD expression was induced with 1mM IPTG for three hours. The cells were resuspended in lysis buffer [50mM Tris-HCl, pH 7.5, 1 mM EDTA, 0.5 M NaCl, 10% glycerol, 1 mM dithiothreitol (DTT), 1 mM phenylmethanesulfonyl fluoride (PMSF), 1 µg/ml leupeptin, 10 µg/ml trypsin inhibitor, and 0.05% deoxycholic acid], and lysed by sonication. The lysate was centrifuged at 39,000g for 30 min. The lysate was then treated with ammonium sulfate at 30%, 50%, and 70% saturation in succession. The pellets were collected by centrifugation at 39,000g for 40 min and the components of each precipitate were examined by SDS polyacrylamide gel electrophoresis. The corresponding precipitates containing the majority of GR DBD were combined and redissolved in 50 mM Tris-HCl (pH 8.0), 50 mM NaCl, 1 mM EDTA, 5 mM DTT, 1 mM ZnSO₄, 1 mM PMSF, 1 µg/ml leupeptin, and 10 µg/ml trypsin inhibitor, and dialyzed against the same buffer overnight. The dialyzed lysate was loaded onto a CM-sepharose column (Pharmacia) and eluted with a linear NaCl gradient (50-600 mM) in 20 mM sodium phosphate buffer (pH 7.6) with 1 mM DTT. The protein concentration of each collected fraction was determined by measuring A_{280} using the extinction coefficient $\epsilon_{280\text{nm}} = 4200 \text{ M}^{-1} \text{ cm}^{-1}$ calculated for tyrosine absorption (Cantor and Schimmel, 1980), and fractions containing proteins were analyzed on a 15% SDS polyacrylamide

gel. The fractions containing GR DBD were combined and concentrated by Centricon YM-3 (Millipore) to about 2 ml. The sample was then loaded onto a Superdex 75 prep grade column (Pharmacia) and eluted with 10 mM HEPES (pH 7.6) with 150 mM NaCl and 1 mM DTT. The protein concentrations of each collected fraction were determined by measuring A_{280} , and the components of fractions containing proteins were resolved on a 15% SDS polyacrylamide gel. The GR DBD containing fractions were transferred to Slide-A-Lyzer® MINI Dialysis Units (3,500 MWCO), and dialyzed against 10 mM HEPES (pH 7.6), 1 mM DTT, 10% glycerol, 10 μ M ZnCl₂, 0.1 mM EDTA overnight. After dialysis, the concentration of each fraction was measured using the Bio-Rad Protein Assay (Bio-Rad). The samples were stored at -80°C.

Preparation of oligonucleotide substrates.

Synthetic oligodeoxyribonucleotides purified by high-pressure liquid chromatography (HPLC) were obtained from Midland Certified Reagent Company, Inc. (Table 2.1). Oligonucleotides were further purified by gel extraction. Briefly, an 80 nucleotide template (F1) that contained a uracil nucleotide within the right half-site of the GRE sequence, and the corresponding undamaged template (F3), were labeled on the 5' ends with [γ -³²P]ATP (Perkin Elmer) using T4 polynucleotide kinase (Invitrogen). The reactions were carried out at 37°C for 10 min and terminated by heating in boiling water for 5 min. To prepare double-stranded DNA substrates, equal molar ratios of an 80 nucleotide template (F2) complementary to F1 and F3 were added to anneal to both templates. The annealed products were then resolved on a 10% native polyacrylamide gel in 0.5 \times TBE (90 mM Tris, 90 mM boric acid, and 1

mM EDTA). The wet gel was exposed to a Phosphorimager screen (Molecular Dynamics) for 30 min; images were then scanned on the Phosphorimager (Molecular Dynamics, Model 445-P90), and printed out on a 100% scale. The printed image was overlaid with the gel, and the bands representing the positions of double-stranded DNA (dsDNA) were excised, cleaved into small pieces, soaked in 300 μ l 0.3 M sodium acetate solution, and shaken on a thermomixer (Eppendorf) overnight at 25°C. In order to quantify the final concentrations of the purified fragments, an aliquot of each fragment solution was mixed with a single-stranded DNA (ssDNA) standard of known concentration, and separated on a 10% native polyacrylamide gel. The gel was vacuum-dried and exposed to a Phosphorimager screen. Each lane was scanned on a Phosphorimager and intensities of DNA bands were quantified with ImageQuANT v4.2 software (Molecular Dynamics). The concentrations of each purified fragment could be calculated from the known concentration of the standard and the ratios of band intensities.

RESULTS

Purification of GR DBD

Rat GR DBD was purified following the scheme described in Materials and Methods. After induction with IPTG (Figure 2.1), the lysate was treated with different saturations of ammonium sulfate. It was found that the majority of GR DBD was precipitated at 50% and 70% saturations (Figure 2.2). The precipitates were combined and first purified on a CM-sepharose column. The total protein concentration (Figure 2.3 A) and purity (Figure 2.3 B) of each fraction were compared, and fractions 15 to 22 were combined and further concentrated. Final purification was carried out using a Superdex 75 prep grade column (Figure 2.4 A). The homogeneous fractions 18 to 24 (Figure 2.4 B) were combined and stored at -80°C .

Purification of DNA substrates

The initial purity of ssDNA substrates received after HPLC purification was ~50% (Figure 2.5). The fragments were then further purified to homogeneity through gel extraction (Figure 2.6 A). After radiolabeling of F1 and F3, 1 pmol of ssDNA was saved as a standard and the rest was used to anneal with F2. The ssDNA was diluted to $0.05\ \mu\text{M}$ and $1\ \mu\text{l}$ was mixed with $1\ \mu\text{l}$ purified dsDNA. Therefore, 0.05 pmol ssDNA was contained in each mixture. After the mixtures were separated on a 10% native polyacrylamide gel (Figure 2.6 B), the concentrations of dsDNA could be calculated from the concentration of the standard and the ratios of band intensities.

DISCUSSION

GR, as a transcription factor, is different from the transcription factor TFIIIA, which has been well studied in the Smerdon lab (Conconi et al., 1999; Kwon and Smerdon, 2003), in multiple ways. The DNA binding domains of both GR and TFIIIA contain zinc finger motifs, but belong to different types. The DBD of GR contains two zinc fingers formed by the tetrahedral co-ordination of two zinc atoms by four pairs of cysteines (Freeman et al., 1988). TFIIIA consists of 9 tandemly repeated C2H2 type zinc fingers, and each zinc atom is coordinated by two cysteines and two histidines (Miller et al., 1985; Brown et al., 1985). The secondary and tertiary structures of GR DBD zinc fingers (Luisi et al., 1991) differ significantly from those of the TFIIIA-type zinc fingers (Klevit et al., 1990; Lee et al., 1989). TFIIIA has a consistent conformation seemingly independent of the presence or absence of DNA (Pavietich and Pabo, 1991). To the contrary, crystallography (Luisi et al., 1991) and NMR (Hard et al., 1990) studies have shown that GR DBD adopts different conformations when free in solution and when bound to DNA. Two GR DBDs bind to one GRE on one face of DNA cooperatively (Luisi et al., 1991), whereas TFIIIA wraps around DNA as a single molecule (Nolte et al., 1998). Binding of TFIIIA is required for transcription initiation of the 5S rRNA gene (Wolffe, 1994), while binding of GR to the enhancer region can modulate transcription rates of target genes, probably by recruiting some remodeling factors (McNally et al., 2000; Fletcher et al., 2000).

In our study, GR DBD is used instead of the entire GR. There are several

reasons for this. First, rat GR requires purification from rat liver cells, while GR DBD can be expressed as a recombinant peptide in *E.coli*. Second, the process of purification for GR is more complicated compared to GR DBD purification. Moreover, a 72 KDa protein always copurifies with GR (Gustafsson et al., 1986) and it is hard to separate from GR. Third, we focused on the effect of GR binding on BER of GRE, and GR DBD contains all the residues required for binding of GR to GRE. It should be noted, however, that GR DBD binds to GRE with ~10-fold lower affinity than the entire GR because GR DBD lacks the region responsible for dimerization in the C-terminal domain (Dahlman-Wright et al., 1992).

As shown in Figure 2.1, the level of induction by IPTG was not very high in these experiments. This could be the normal level of induction for GR DBD from the plasmid pGR440 in the *E.coli* strain BL21 [DE]/pLysS, although it might also be possible that optimal conditions of GR DBD expression in *E.coli* were not used. Multiple factors can affect the level of expression, such as temperature, cell density used to initiate induction, and incubation time of induction. Ammonium sulfate precipitation was the first purification step used to remove some contaminating proteins. It was noted that ammonium sulfate should be added to the cell lysate very slowly, otherwise the local concentration of salt can be higher than desired and the protein of interest can be precipitated at overall lower ammonium sulfate concentrations. After purification on a CM-sepharose column, the sample was further purified by a Superdex 75 prep grade column. This second step of purification was necessary to remove a contaminating nuclease. GR DBD samples after CM-sepharose

column purification partially degraded DNA substrates (data not shown). However, after the second column step, GR DBD was purified to homogeneity and contained no nuclease activity.

DNA substrates in our present study contain just the distal MMTV I GRE. Using the entire MMTV-LTR containing four GREs will give additional complexity to our model system (e.g., in analyzing the effect of dU on GR DBD binding, it is harder to measure the change of the K_d value since there are multiple binding sites for GR DBD in the entire MMTV-LTR.). As discussed above, MMTV I GRE offers the greatest contribution to the overall transcriptional activation. Therefore, study of this GRE should provide more information about the overall function of MMTV-LTR than the other GREs. Gel purification of HPLC-purified fragments was necessary for the repair assays. For instance, UDG/APE1 digestions were measured as the appearance of a shorter product band after denaturing gel electrophoresis. After a short incubation time, only a weak band resulting from UDG/APE1 digestions could be visualized. Thus, if the contaminating bands were present, it was hard to distinguish the cleavage reaction bands from the contaminating bands.

Taken together, GR DBD and DNA substrates were purified to homogeneity, and ready to be used for binding and repair assays.

FIGURES AND TABLES

Abbreviation	Sequence
F1:	5'-TTGCGGTTCCAGGGTTAAATAAGTTTATG <u>GTTACAAACTGTT</u> <u>U</u> TTAAAA CGAGGATGTGAGACAAGTGGTTTCCTGAC-3'
F2:	5'-GTCAGGAAACCACTTGTCTCACATCCTCGTTTTA <u>AGAACAGTT</u> <u>TGTAACC</u> ATAAACTTATTTAAACCCTGGGAACCGCAA-3'
F3:	5'-TTGCGGTTCCAGGGTTAAATAAGTTTATG <u>GTTACAAACTGTT</u> <u>CTTAAAA</u> CGAGGATGTGAGACAAGTGGTTTCCTGAC-3'

Table 2.1 Oligonucleotide Sequences and Abbreviations. Both half-sites of GRE in each oligonucleotide are underlined. The site of dU incorporation is indicated in red.

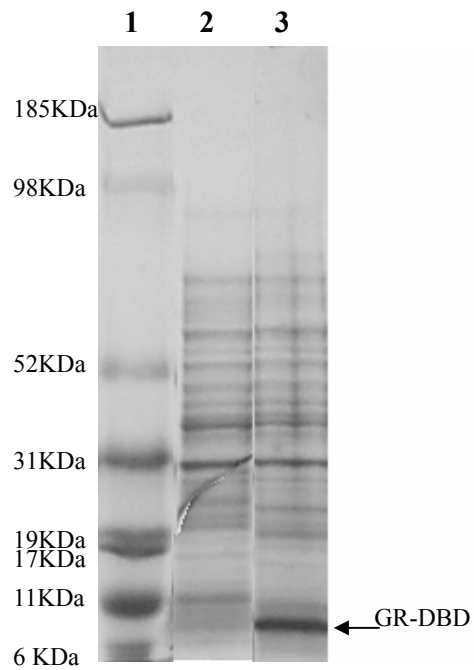


Figure 2.1 SDS Gel of Cell Lysates before and after IPTG Induction. Lane numbers are as follows: **1:** Mw Marker; **2:** Before IPTG induction; **3:** After IPTG induction. Arrow indicates the position of GR DBD.

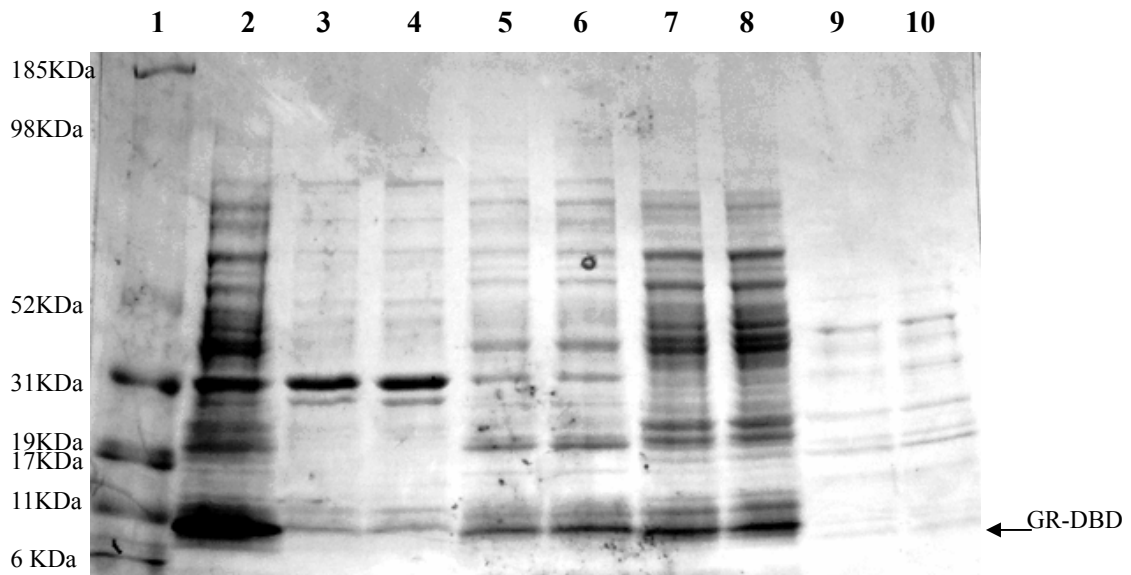
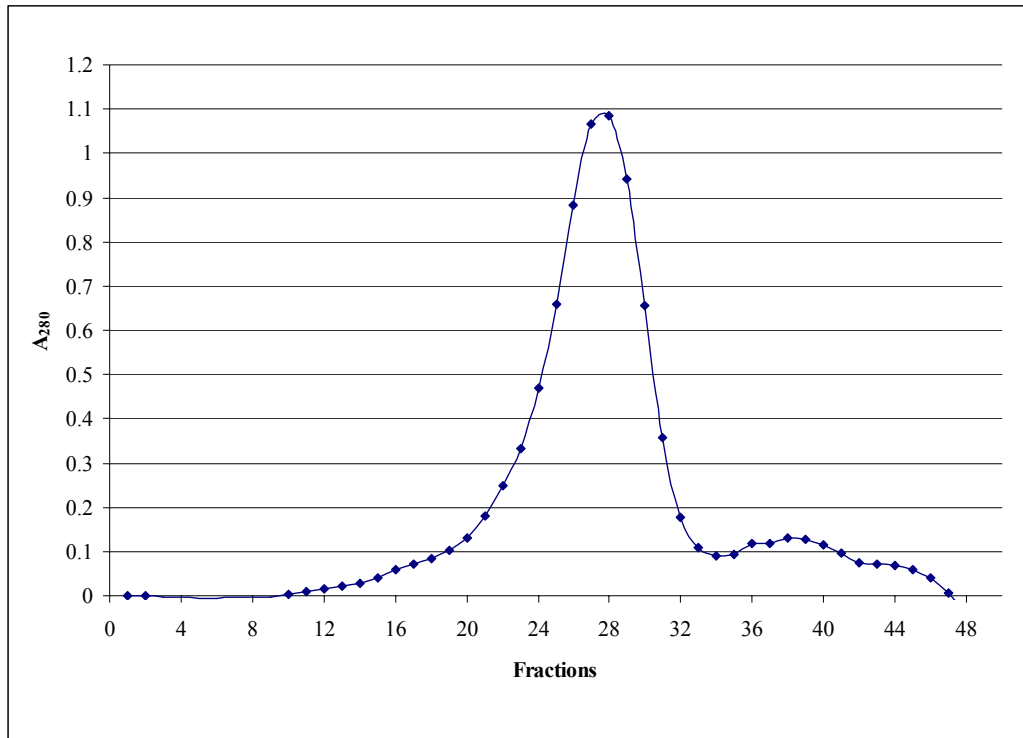


Figure 2.2 SDS Gel of Ammonium Sulfate Precipitation. Lane numbers are as follows: **1:** Mw Marker; **2:** Cell lysate after IPTG; **3 & 4:** 30% ammonium sulfate pellet; **5 & 6:** 50% ammonium sulfate pellet; **7 & 8:** 70% ammonium sulfate pellet; **9 & 10:** 70% ammonium sulfate supernatant. Arrow indicates the position of GR DBD.

A



B

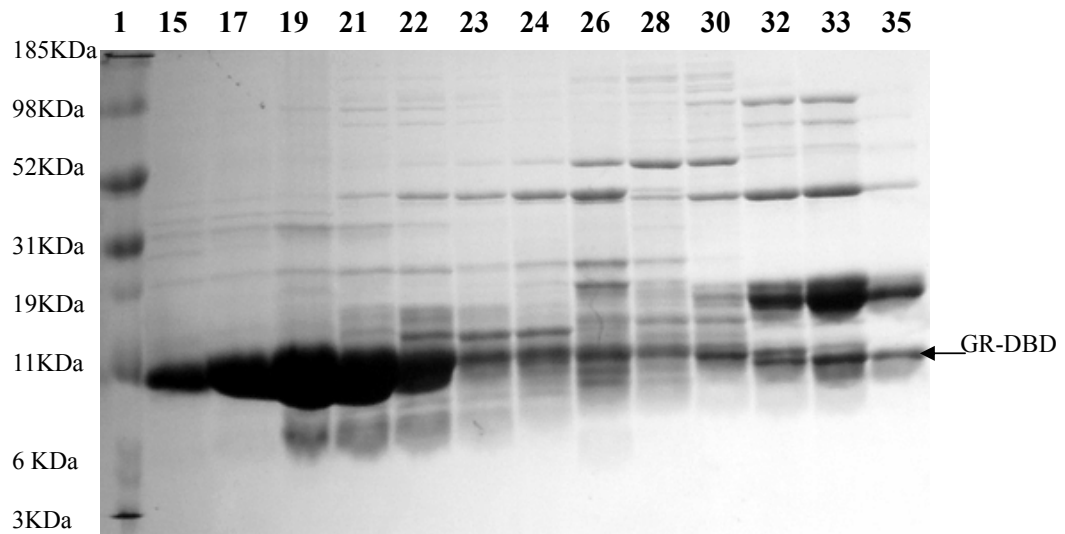
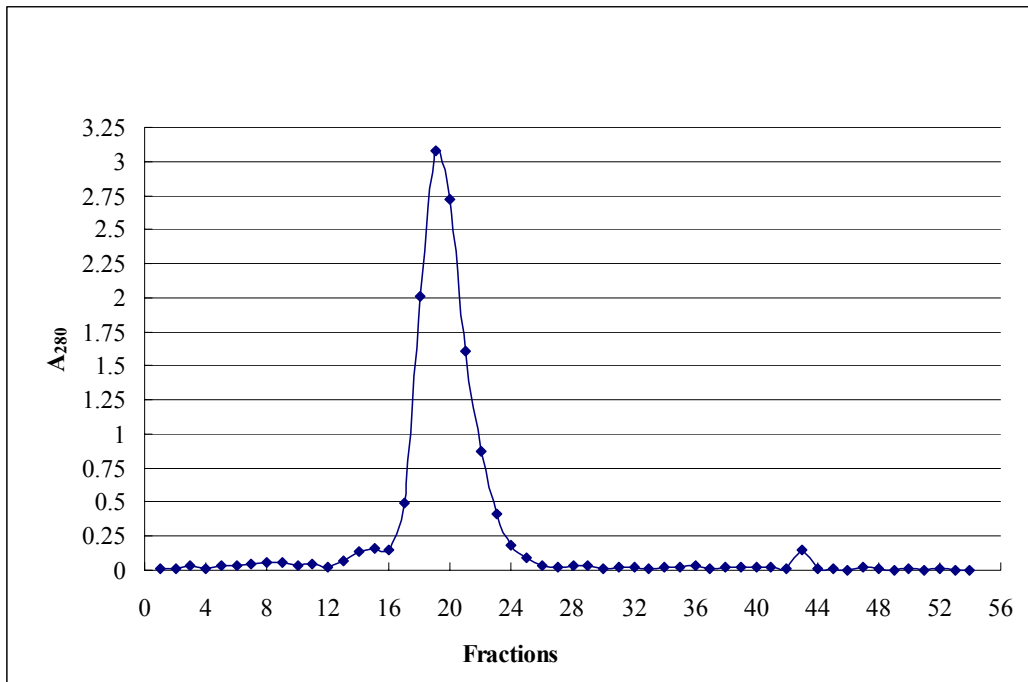


Figure 2.3 Purification on a CM-Sepharose Column. (A) Elution profile. Purification was carried out using a 100ml linear gradient from 100mM NaCl to 1M NaCl. (B) SDS-PAGE showing the purity of different fractions. Lane numbers are as follows: 1: Mw Marker; The remaining lane numbers correspond to the numbers of collected elution fractions. Arrow indicates the position of GR DBD.

A



B

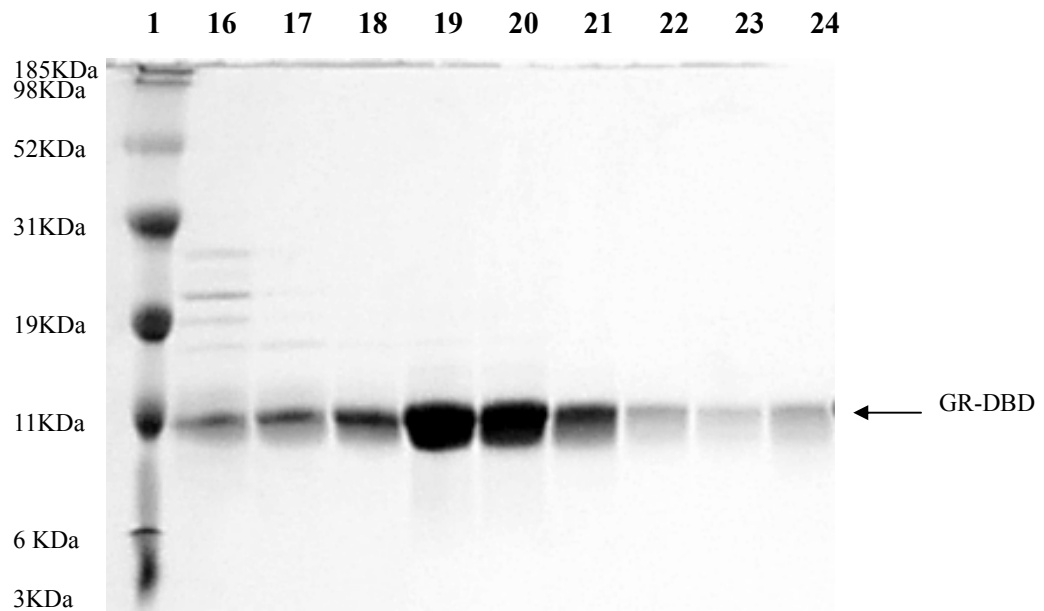


Figure 2.4 Purification on a Superdex 75 Prep Grade Column. (A) Elution profile. (B) SDS-PAGE showing the purity of different fractions. Lane numbers are as follows: 1: Mw Marker; The remaining lane numbers correspond to the numbers of collected fractions. Arrow indicates the position of GR DBD.

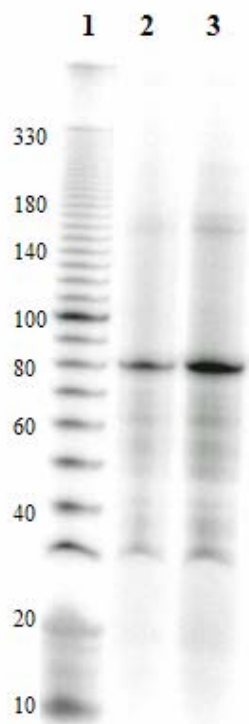
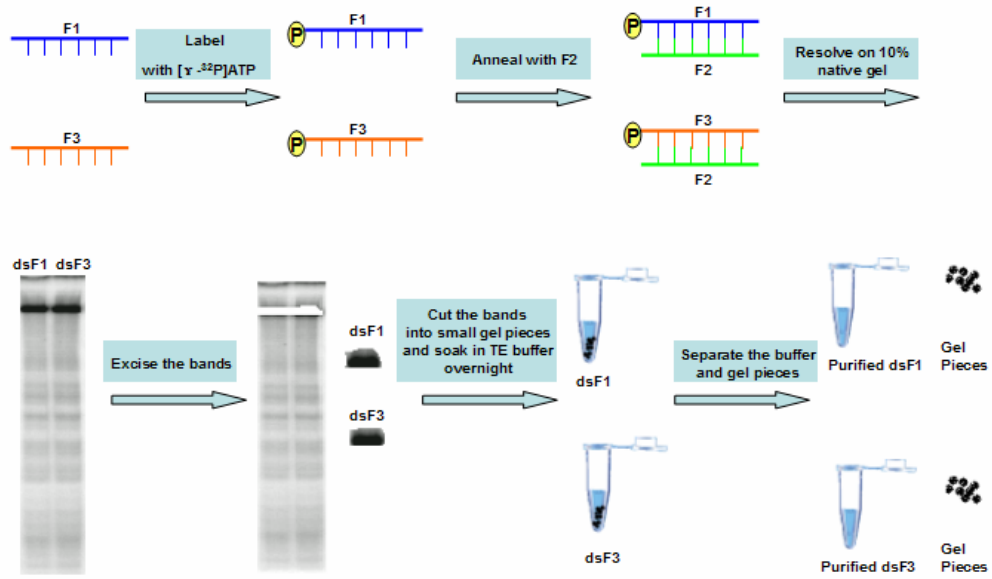


Figure 2.5 Urea Gel of Oligonucleotides before Purification. Lane numbers are as follows: **1**: 10bp DNA Marker; **2**: ssF1; **3**: ssF3.

A

Process of Gel Purification:



B

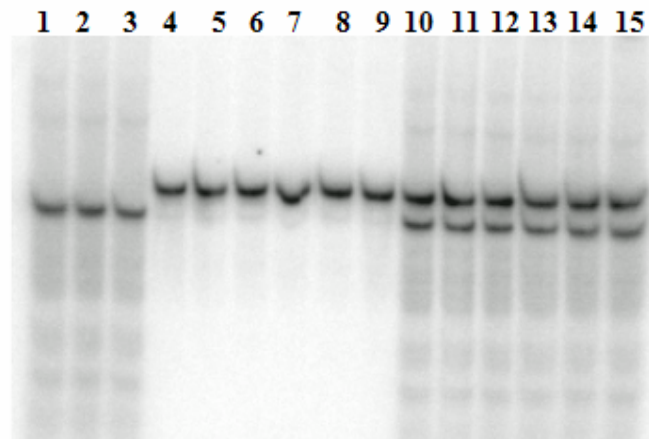


Figure 2.6 Gel Extraction and Quantification of Purified DNA. (A) Process of gel extraction. F1 and F3 were annealed separately to F2 to form 80bp dsDNA substrates. dsF1 and dsF3 were separated from ssDNA and other small contaminating DNA on a native gel (10% polyacrylamide in $0.5 \times$ TBE). The corresponding bands were then excised and cut into small pieces. The gel pieces were dissolved in 500 μ l 0.3M Sodium Acetate overnight. The small gel pieces were then removed by centrifugation and 1ml 100% ethanol was added to the supernatant to pellet DNA. (B) Native gel for quantification of purified dsDNA. Lane numbers are as follows: Lane 1, 2, 3: ssDNA of known concentration; Lane 4, 5, 6: Purified dsF1; Lane 7, 8, 9: Purified dsF3; Lane 10, 11, 12: Mixture of 1 μ l ssDNA and 1 μ l dsF1; Lane 13, 14, 15: Mixture of 1 μ l ssDNA and 1 μ l dsF3. The gel was exposed to a Phosphorimage screen and the intensities of resolved bands on the gel were quantified using ImageQuaNT v4.2 software. Since the concentration of ssDNA and the ratios of intensity of ssDNA to that of dsDNA were known, the concentrations of dsDNA could be calculated.

REFERENCES

- Brown, R.S., Sander, C., and Argos, P. (1985) *FEBS Lett.* 186, 274-274.
- Conconi, A., Liu, X., Koriazova, L., Ackerman, E.J., and Smerdon, M.J. (1999) *EMBO J.* Mar 1; 18(5), 1387-1396.
- Dahlman-Wright, K., Wright, A.P.H., and Gustafsson, J. (1992) *Biochemistry* 31, 9040-9044.
- Fletcher, T.M., Ryu, B., Baumann, C.T., Warren, B.S., Fragoso, G., John, S., and Hager, G.L. (2000) *Molecular and Cellular Biology* Sept; 6466-6475.
- Freeman, L.P. et al. (1988) *Nature* 334, 543-546.
- Gustafsson, J., Carlstedt-Duke, J., Wrangé, Ö., Okret, S., and Wikström, A. (1986) *J. Steroid Biochem.* 24(1), 63-68.
- Hard, T. et al. (1990) *Science* 249, 157-160.
- Klevit, R.E., Herriott, J.R., and Horvath, S.J. (1990) *Proteins* 7, 215-226.
- Kwon, Y. and Smerdon, M.J. (2003) *J Biol Chem.* Nov 14; 278(46), 45451-45459.
- Lee, M.S., Gippert, G.P., Soman, K.V., Case, D.A., and Wright, P.E. (1989) *Science* 245, 635-637.
- Luisi, B.F., Xu, W.X., Otwinowski, Z., Freedman, L.P., Yamamoto, K.R., and Sigler, P.B. (1991) *Nature* 352, 497-505.
- Lundback T, Zilliacus J, Gustafsson JA, Carlstedt-Duke J, and Hard T. (1994) *Biochemistry* May 17; 33(19), 5955-5965.
- McNally, J.G., Müller, W.G., Walker, D., and Hager, G.L. (2000) *Science* 287, 1262-1264.
- Miller, J., McLachlan, A.D., and Klug, A. (1985) *EMBO J.* 4, 1609-1614.
- Nolte, R.T., Conlin, R.M., Harrison, S.C., and Brown, R.S. (1998) *Proc. Natl. Acad. Sci. USA* 95, 2398-2443.
- Pavietich, N.P. and Pabo, C.O. (1991) *Science* 252, 809-817.
- Wolffe, A.P. (1994) *J. Cell Science* 107, 2055-2063.

CHAPTER III

Effects of Glucocorticoid Receptor Binding *In Vitro* on Base Excision Repair of Deoxyuridine in the Glucocorticoid Response Element

SUMMARY

We have investigated the effect of glucocorticoid receptor (GR) binding on base excision repair (BER) *in vitro*. Initially, the interaction of the GR DNA binding domain (GR DBD) with undamaged and uracil-containing GRE (dU-GRE) DNA was examined using a gel mobility shift assay. As expected, the GR DBD binding affinity for the dU-GRE fragment was very similar to that of the undamaged fragment, ~ 0.8 nM. We then examined the efficiency of individual enzymatic steps of BER at specific uracil incorporation sites in the GRE following binding of GR DBD. We found that access of uracil DNA glycosylase (UDG) and apurinic/apyrimidinic endonuclease (APE) is decreased by almost 20-fold following binding of GR DBD. On the other hand, incorporation of [α -³²P]dCTP by DNA polymerase beta (pol β) was decreased ~2.5-fold after 4 h incubation following GR DBD binding. This latter observation is surprising, since we have observed a complete lack of activity by pol β on nucleosome core DNA (Beard et al. 2003). Thus, these results enhance our understanding of the mechanism of DNA damage recognition and repair in protein-DNA complexes.

INTRODUCTION

DNA lesions resulting from exogenous and endogenous genotoxic agents are required to be removed by a series of repair pathways to avoid genomic instability, cancer or cell death. Efficiency of repair can be modulated in multiple ways; one of them is binding of proteins to DNA, which can shield lesions from the repair machinery. Examples of such proteins are transcription factors or histone octamers. Slow repair of promoter regions caused by binding of transcription factors has been observed both *in vivo* (Gau et al., 1994; Tu et al., 1996; Tommasi et al., 2000) and *in vitro* (Conconi et al., 1999). The relationship between NER and binding of the transcription factor TFIIIA has been well studied in the Smerdon lab. Former work has shown that binding of TFIIIA to the 5S ribosomal RNA gene (rRNA) can be affected by a single cyclobutane thymine dimer (CTD) at specific sites in the internal control region (ICR) where TFIIIA binds (Kwon and Smerdon, 2003). On the other hand, binding of TFIIIA to the 5S rRNA gene can also decrease the NER rate of CTDs in the ICR (Conconi et al., 1999).

Furthermore, it was shown that enzymes of the base excision repair (BER) pathway carry out their catalytic activities with significantly reduced efficiency on nucleosome substrates, containing deoxyuradine (dU), *in vitro* (Nilsen et al., 2002, Beard et al. (2003) and can even be completely blocked by tight histone binding at strong nucleosome positioning sequences (Beard et a., 2003).

In the present study, we examined how binding of another well-studied

transcription factor, the glucocorticoid receptor (GR), affects BER in its recognition sequence, the glucocorticoid response element (GRE). Upon binding of hormone, inactive GR transforms into active GR which then forms dimers, translocates to the nucleus, binds to GREs and triggers transcription activation or repression. GR, which has a M_r between 85,000 and 95,000 (Rousseau, 1984), has three major functional domains—an N-terminal domain involved in activation of transcription, a central DNA-binding domain (DBD), and a C-terminal ligand-binding domain. The determinants for interaction with DNA reside entirely within the DBD which includes a highly conserved 66-68-amino acid segment (Green and Chambon, 1987; Freeman et al., 1988; Dahlman et al., 1989). Therefore, to simplify the purification process, GR DBD was used in these experiments instead of the entire GR. The 15 bp GRE can be a perfect or imperfect palindrome, which has two inverted repeat sequences separated by three nucleotides. The right half-site of GRE is always TGTTCT, but the left half-site can differ. The differences in sequences can cause differences in their ability to function as response elements (Ham et al. 1988).

The mouse mammary tumor virus long terminal repeat (MMTV-LTR), which contains four GREs, has served as the prototype for studies developing the conceptual framework of the molecular mechanisms of glucocorticoid hormone action. In the present study, an 80 bp DNA segment of the MMTV-LTR containing the distal full-length GRE (MMTV I GRE) was used as the DNA substrate. The MMTV I GRE offers the greatest contribution to the overall transcriptional activation; therefore, study of this GRE should provide more clues to the overall function of MMTV-LTR

than the other GREs.

In this study, we examined BER of a dU in DNA, which can arise from spontaneous deamination of cytosine, errors in replication, or attacks by small molecules such as bisulfate (Chen and Shaw, 1993) and nitrous acid (Wink et al., 1991). Approximately 200 cytosine deamination events occur each day in a genome of 10^{10} base pairs, and deamination is expected to occur 1,000 times faster in single-stranded DNA (ssDNA) than in double-stranded DNA (dsDNA), making it a significant event in actively transcribed genes and replication forks (Lindahl, 1979). Additionally, over 10,000 deoxyuridine incorporation events occur per replication cycle in a genome of 10^{10} base pairs (Lindahl, 1979). Misincorporation of uracil produces a G·U base pair which leads to a G·C→A·T transition after a round of DNA replication. This transition can disrupt sequence specific DNA recognition by gene regulatory proteins (Verri et al., 1990), or change the codons of specific genes, all of which will affect normal cell functions (Doetsch, 2002).

The entire BER pathway can be reconstituted *in vitro* with purified enzymes (Srivastava et al., 1998). In our study, we divided the BER pathway into its individual components [uracil DNA glycosylase (UDG), apyrimidinic/apurinic endonuclease (APE), and DNA polymerase β (pol β)] and tested how the catalytic activities of these enzymes are modulated by GR DBD binding.

MATERIALS AND METHODS

Gel mobility shift assays.

Labeled damaged (dU-containing) and undamaged DNA substrates at varying concentrations were incubated with GR DBD in 20 μ l of GR DBD binding buffer [10 mM HEPES, pH 7.9, 2.5 mM $MgCl_2$, 0.05 mM EDTA, 10% glycerol, 50 mM NaCl, 0.1% Triton X-100, 1 mM DTT, 2.5 ng/ μ l poly (dI·dC), and 10 μ M $ZnCl_2$] at room temperature for 30 min. Incubation of GR DBD with DNA resulted in formation of a protein-DNA complex, which was separated from free DNA on a 10% native polyacrylamide gel run in 0.5 \times TBE buffer at 10 V/cm for about 2 hours. The gel was vacuum-dried and exposed to a Phosphorimager screen to visualize DNA bands, as described in Chapter II. Intensities of DNA bands were quantified using ImageQuANT v4.2 software (Molecular Dynamics). Concentrations of bound and free DNA were calculated from the intensities of DNA bands and the total concentration of DNA. The ratio of the concentration of bound DNA to that of free DNA *versus* the concentration of bound DNA was plotted and the data fit with a least-squares linear regression to obtain a K_d value (Clemens 1994), using the following equation:

$$\frac{[\text{bound}]}{[\text{free}]} = ([GR\ DBD]_{\text{total}} - [\text{bound}]) \times \frac{1}{K_d}$$

Methylation protection in GR DBD-DNA complexes.

End-labeled 80 bp damaged and undamaged DNA substrates (0.5 pmol) were

incubated with 3.2 pmol of GR DBD in 40 μ l of the binding buffer at room temperature for 30 min. One μ l of 8% dimethyl sulfate (DMS) in ethanol was added to the reaction mixtures and incubated at room temperature for 2 min, to methylate primarily guanine residues. Subsequently, the samples were loaded onto 10% native polyacrylamide gels and run for 2 h at 100 V until bound and free DNA were well separated. Both bound and free DNA bands were excised, cleaved into small pieces, and soaked in 300 μ l of 0.3 M sodium acetate solution at 25°C overnight to elute the DNA. The DNA was ethanol-precipitated, re-dissolved in 70 μ l of 10% piperidine and incubated at 90°C for 30 min to depurinate and cleave the phosphate backbone at methylated guanine residues. The samples were then dried and washed three times with 30 μ l of H₂O. Finally, the DNA samples were dissolved in 10 μ l of 2 \times denaturing solution [95% (v/v) formamide, 10 mM EDTA (pH 8.0), 0.1% (w/v) bromophenol blue, 0.1% (w/v) xylene cyanol], and heated in boiling water for 10 min. After heating, the samples were chilled on ice immediately. The cleaved DNA fragments were resolved on a sequencing gel (0.4 mm thick \times 17 cm wide \times 60 cm long) containing 7 M urea, 10% polyacrylamide and TBE buffer for 2 h at 65 W. After electrophoresis, the gel was dried and exposed to a Phosphorimager screen to visualize DNA bands as previously described.

Uracil DNA glycosylase and AP endonuclease digestions.

The UDG and APE1 reaction mixtures contained 50 mM HEPES (pH 7.5), 2 mM DTT, 0.2 mM EDTA, 100 μ g/ml BSA, 10% glycerol, 5 mM MgCl, and 4 mM

ATP. Two sets of experiments were performed. A saturating amount of GR DBD was added to one set of reaction mixtures to form GR DBD-DNA complexes. The other set contained only naked DNA. Reactions were initiated by adding 1/60 unit of *E. coli* UDG (New England Biolabs) and 1/10 unit of APE (New England Biolabs) to 20 μ l reaction mixture. Incubation was at 37°C for 5 to 30 min. Aliquots were removed at appropriate times and treated with phenol to terminate the reactions. Double-stranded DNA was denatured by addition of 0.2 N NaOH, followed by heating in boiling water for 10 min. Subsequently, DNA was ethanol-precipitated and separated on a 7M urea gel (10% polyacrylamide and 0.5% bisacrylamide) in 0.5 \times TBE. The gel was then dried and exposed to a Phosphorimager screen to visualize DNA bands as previously described.

DNA polymerase β synthesis.

Pol β was obtained as a free gift from Dr. Samuel Wilson. The 20 μ l reaction mixtures for pol β synthesis contained the same buffer as described above except for the addition of 0.1 μ l [α -³²P]dCTP. Similarly, two sets of experiments were performed. A saturating amount of GR DBD was added to one set of reaction mixtures to form GR DBD-DNA complexes. The other set contained just naked DNA. Initially, 1/6 unit of UDG and 1 unit of APE were added to 20 μ l reaction mixtures to start the digestions. After 1.5 hours, 10 nM pol β was added to the reaction mixtures. The reactions were terminated at various time points by phenol extraction and heating at 100°C for 10 min. After ethanol precipitation, the incorporation of [α -³²P]dCTP was

detected by separation of DNA samples on a 7 M urea gel (10% polyacrylamide and 0.5% bisacrylamide in 0.5 × TBE), which was then dried and exposed to a Phosphorimager screen to visualize DNA bands as described earlier.

RESULTS

Binding of GR DBD to intact and uracil-incorporated DNA.

In these experiments, the GR DBD-binding affinities of intact and dU-GRE DNA were compared by gel mobility shift assays. These assays were performed either by titration of a fixed amount of DNA with increasing amounts of protein (Figure 3.2) or by titration of a fixed amount of protein with increasing amounts of DNA (Figure 3.3). It has been shown in a previous study on the GRE of the tyrosine amino transferase (TAT) gene promoter, GR DBD binds first to the downstream GRE half-site (TGTTCT), then subsequently occupies the upstream GRE half-site (TGTACA) (Tsai et al., 1988). Since only the first two bases in the upstream half-site (GTTACA) of the MMTV I GRE used in this study are reversed compared to the TAT GRE, we expected that the GR DBD might bind the MMTV I GRE in a similar manner. Indeed, the expected pattern was observed. At low concentrations, GR DBD bound to only one half-site of GRE, with or without the dU base (Figure 3.2). A more slowly migrating form of protein-DNA complex (arrows in Figure 3.2) was observed only at high concentrations of GR DBD (Figure 3.2, panels A and B, lane 8).

To gain further insight into the sequential order of GR DBD binding to both half-sites of GRE, we conducted methylation protection experiments. With this analysis, reduction in cleavage by piperidine following DMS methylation at specific sites identifies guanines involved directly in protein binding. We observed that cleavage at the G residues in the right half-sites of GRE of the undamaged and

damaged DNA substrates was reduced dramatically following GR DBD binding, indicating the selective occupation of that half-site by GR DBD (Figure 3.4, asterisks).

Since DNA concentrations can be estimated more accurately than protein concentrations in these experiments, DNA titration was used to determine K_d 's, as described by Dahlman-Wright et al. (1992). Gel retardation assays, followed by Scatchard analysis, were performed to evaluate the effect of uracil incorporation in GRE on protein binding (Figure 3.3). We found that the GR DBD binding affinity of the dU-GRE fragment is very similar to that of the intact fragment, ~ 0.8 nM. Thus, the change from C to U in the crucial half-site of the GRE has little effect on the binding affinity of GR DBD.

Effect of GR DBD binding on the cleavage reaction of uracil DNA glycosylase and AP endonuclease.

Two sets of experiments were performed to test the cleavage reaction of uracil DNA glycosylase and AP endonuclease on the MMTV I GRE. One set contained just the naked DNA, while the other set contained a mixture of DNA and a saturating amount of GR DBD. As shown in Figure 3.5 C, all DNA in the GR DBD-containing set of experiments are in GR DBD-DNA complexes. As mentioned in the introduction, UDG catalyzes the hydrolytic removal of the target base so as to form an apurinic/aprimidinic (AP) site. APE then cleaves 5' to the abasic sugar to produce a single strand break which can be visualized as a lower molecular weight band on a

denaturing gel (Figure 3.5 A, band C). As can be seen in Figure 3.5 A, generation of this band during increasing digestion times is significantly retarded in the GR DBD-DNA complexes (compare lanes 1-6 with lanes 7-12). The degree of retardation was determined by plotting the percentage of uncut full-length DNA (Figure 3.5 A, band FL) in both sets of experiments *versus* the incubation time. From the slopes of these digestion curves, the time course of the reaction of UDG and APE1 is decreased almost 20-fold following binding of GR DBD.

Effect of GR DBD binding on DNA polymerase β synthesis.

It has been shown that pol β performs strand elongation prior to removal of the 5'-dRP moiety (Srivastava 1998). Because this order of reaction has been well characterized, only the initial step of dCTP incorporation by pol β was assayed. At high concentrations of UDG and APE, digestions for 1.5 h proceeded to completion on both the naked DNA and protein-DNA complexes (Figure 3.6A), giving a fully nicked population of fragments for the pol β reaction in each case. Incorporation of [α -³²P]dCTP into the MMTV I GRE by pol β was decreased ~2.5-fold after 4 h incubation following GR DBD binding (Figure 3.6 B&C).

DISCUSSION

GR DBD binding to intact and dU-containing DNA.

The GRE sequence used in this study is the distal GRE of the MMTV-LTR (MMTV I GRE) (Figure 3.1). In comparison to the TAT GRE, there are two base differences at positions -7 (left) and -6 (left). However, it has been shown that GR displays a higher affinity for GREs with a guanine at position -6 (left) than any other base (Nordeen et al., 1990; Nelson et al., 1999). Furthermore, the crystal structure of a GR DBD-DNA complex identified this G (-6, left) in the top strand, and the G (-6, right) in the bottom strand, as acceptors of one direct and one water-mediated hydrogen bonds from an invariant Lys 461 (Luisi et al., 1991; Figure 3.7). According to Necela and Cidlowski (2004), mutation of T (-6, left) to G in MMTV I GRE strongly increases (~ 8 fold) transcriptional activation by GR. Assuming that transcriptional activation reflects the binding affinity of GR to the GRE, these observations indicate that GR binding to the left half-site can be greatly facilitated by T (-6, left) to G mutations. Due to the strong dimerization of GR upon binding of hormone, binding of GR to the right half-site serves to vastly increase the local concentration of receptor in the vicinity of the left half-site, thereby facilitating binding of the second receptor.

The GR DBD is a monomer in solution, and binding of the second GR DBD to the GRE requires a change of conformation induced by cooperative interactions with the DNA-bound GR DBD, DNA phosphates and DNA bases. Because GR DBD

lacks the region responsible for dimerization in the C-terminal domain, GR DBD binds to the left half-site of GRE with ~10-fold lower affinity than the intact GR (Dahlman-Wright et al., 1992). In addition, the mutation of G (-6, left) to T causes the loss of hydrogen bonding between G (-6, left) and GR DBD (see Figure 3.7). For these reasons, binding of the second GR DBD to the left half-site is greatly diminished in our system, making the binding pattern different from that seen for the TAT GRE, where GR DBD binding to the downstream half-site of GRE facilitates the binding of the second GR DBD molecule, and two distinct bands are clearly detected in the EMSA gels (Tsai et al., 1988). For MMTV I GRE used in our study, the binding of the second molecule is very weak, and a faint band can only be seen when the protein concentration is very high. This simplifies our system to a one-ligand, one-receptor system at relative low protein concentrations, and interpretation of the Scatchard analysis is straightforward.

Methylation at the N-7 positions of all three G residues (Figure 3.1, denoted by open arrows) in the MMTV I GRE prevents binding of the receptor (Scheidereit and Beato, 1984). It is therefore highly likely that sequence recognition involves direct contacts with the G·C base pair that is hindered after methylation by DMS (Scheidereit and Beato, 1984). Furthermore, it has been reported that transcription of the bacterial chloramphenicol acetyltransferase (CAT) gene is completely abolished by mutations at T (4, right) and T (5, right) positions, and greatly reduced by mutating T (5, right) to C (Klock et al., 1987). Taken together, the above findings demonstrate that G (3, right), T (4, right) and probably T (5, right) are characteristic of functional

GREs. This conclusion is consistent with the results obtained from the study of co-crystal structures of GR DBD and GRE (Luisi et al., 1991). G (3, right) makes two hydrogen bonds with the invariant Arg 466 of GR. The methyl group of T (4, right) makes a favorable van der Waals contact with the side chain of the conserved Val 462. Moreover, T (5, right) and Lys 461 are linked via a hydrogen bond mediated by a water molecule. These three bases all reside in the major groove of the right-half site of the GRE. In addition to these bases in the TGTTCT strand, G (-6, right) in the complementary strand plays an important role in GR DBD binding by accepting one direct and one water-mediated hydrogen bond from the invariant Lys 461 (Luisi et al., 1991). Conversely, there are no direct protein contacts to the bases in the intervening minor groove. There are only contacts made to the phosphate backbone by GR DBD at the ends of both half-sites and the regions closest to the dyad, , and only subtle changes in GRE function are observed following mutations in these regions (Nordeen et al., 1990).

In the present study, C (6, right) was mutated to U. According to the crystal structure, C (6, right) is twisted away from the GR DBD binding site. In addition, the supporting evidence (discussed above) shows no interaction between this base and the protein. Our results demonstrate that there is no change in the binding affinity of GR DBD caused by this mutation, and this conclusion agrees well with all previous studies.

Although the C (6, right) to U mutation does not change GR DBD binding, if not repaired after replication, the G·C pair of one copy of nascent dsDNA will change

to an A·U pair. As discussed before, G (-6, right) in the opposite strand plays an important role in GR DBD binding. If G (-6, right) is mutated to A, it is speculated that the GR DBD binding is decreased. Indeed, the “relative inducibility” change caused by this G (-6, right) to A mutation was analyzed by CAT gene expression and found to reduce the expression level of this gene (Nordeen et al., 1990).

Effects of GR DBD binding on BER.

The first step of BER is the damage-specific recognition by DNA glycosylases (Sancar et al., 2004). In this thesis, we used the *E.coli* uracil DNA glycosylase (UDG) which is closely related to the human UDG, having 73.3% similarity (Olsen et al., 1989). UDG cleaves the glycosyl bond between a target uracil and the deoxyribose sugar, hence generating an AP site. As mentioned earlier, AP sites can have much more deleterious effects on cells than base damage. However, amazingly, it has been found that UDG binds to AP sites more tightly and more rapidly than to uracil-containing DNA, and thus may protect cells from AP site toxicity via steric hindrance of APE cleavage (Stivers et al., 1999). It is postulated that other damage-specific glycosylases also possess this ability, and may remain bound to, or rapidly rebind, AP sites until replaced by APE (Stivers et al., 1999).

Before base flipping, the k_{off} for UDG binding to uracil containing DNA is very similar to that of the nonspecific binding (i.e. in a range of $\sim 500\text{-}1000\text{ s}^{-1}$; Stivers et al., 1999). This fast off-rate reflects a relatively short residence time on the DNA. Therefore, it is not possible to detect UDG-DNA complexes by gel mobility shift

assay (Stivers et al., 1999). Kinetic studies also show that UDG binding occurs by a two-step mechanism. First, UDG forms a weak non-specific complex with DNA, essentially by diffusion ($K_d \approx 1.5\text{-}3 \mu\text{M}$), and then uracil flipping occurs rapidly. The apparent dissociation constant for UDG binding to dsDNA containing a uracil is $\sim 50\text{-}80 \text{ nM}$ (Stivers et al., 1999).

We measured an apparent K_d for GR DBD binding to DNA of $\sim 0.8 \text{ nM}$. Therefore, in the presence of saturating amounts of GR DBD, it is hard for UDG to gain access to uracil within the GRE. Notably, previous data shows that APE1 significantly increases the uracil excision efficiency of UDG (Parikh et al., 1998). Since it appears there is no direct interaction between these two enzymes, it is proposed that this effect is caused by competition for binding to AP sites, and APE1 may literally pry off UDG from AP sites since it has more extensive and stronger interactions with AP sites (Parikh et al., 1998). The dissociation rate for APE binding to AP sites is very slow ($K_{\text{off}} \approx 0.04 \text{ s}^{-1}$) and the association rate constant is about $5 \times 10^7 \text{ M}^{-1}\text{s}^{-1}$ (Strauss et al., 1997). The corresponding equilibrium dissociation constant is, therefore, 0.8 nM (Strauss et al., 1997). Taken together, we can conclude that UDG cleavage is the rate-limiting step in our experiments when GR DBD is present. Once the uracil is cleaved, APE1 can perform its function with moderate interference from GR DBD since they have similar K_d values. These speculations are in line with previous research by Nilsen et al. (2002) and Beard et al. (2003), who found that UDG is a rate-limiting step for repair of nucleosome core particles *in vitro*. Nilsen et al. has found that the activity of UDG in nucleosomes containing the 5S rRNA gene is

reduced 3- to 9-fold when compared with naked DNA, while APE1 can incise 5' to the AP site efficiently in both naked DNA and nucleosomes. Dr. Beard also found that UDG digestion alone on G·U containing nucleosomes shows the same trend as the combined action of UDG and APE, which indicates that the initial-limiting step in BER is UDG catalysis (Beard, 2003).

We found that, as expected, after UDG and APE1 concentrations are increased to high levels, the UDG/APE1 digestions go to completion in both naked DNA and GR DBD-DNA complexes. Subsequently, pol β was added and, incorporation of [α -³²P]dCTP was decreased ~2.5-fold after 4 h incubation following GR DBD binding. This is in contrast to the lack of activity we observed previously in nucleosome core particles (Beard et al., 2003), and the greatly reduced activity seen by Nilsen *et al.* (2002) in a similar *in vitro* system. A possible explanation for these disparities, may involve the differences in binding abilities of GR DBDs and histone octamers to DNA. Histone octamers make extensive contacts with DNA along the surface of core particles, and access of UDG and APE to DNA was hypothesized to depend on the “torsional flexibility” of DNA on the histone surface (Beard et al., 2003). Therefore, these enzymes may only destabilize histone-DNA interactions locally, without completely releasing the DNA from octamers (Nilsen et al., 2002). The differences observed with nucleosomes in the two previous reports can be explained by the stronger binding affinity of DNA containing TG motifs to the histone octamer (Beard et al., 2003) as compared to the 5S rRNA gene (Nilsen *et al.* 2002; see discussion in Beard et al., 2003). To the contrary, the interaction between GR DBD and DNA is

interrupted by the access of UDG as well as APE. Furthermore, yeast two-hybrid experiments have demonstrated a direct interaction between APE and pol β , which agrees well with results of gel retardation assays (Bennett et al., 1997). Therefore, APE acts as a loading factor for pol β onto non-incised AP sites in DNA (Bennett et al., 1997).

Taken together, this study reveals that binding of GR can retard BER of a gene promoter region *in vitro*. These results enhance our understanding of the mechanisms of DNA damage recognition and repair in protein-DNA complexes.

FIGURES AND TABLES

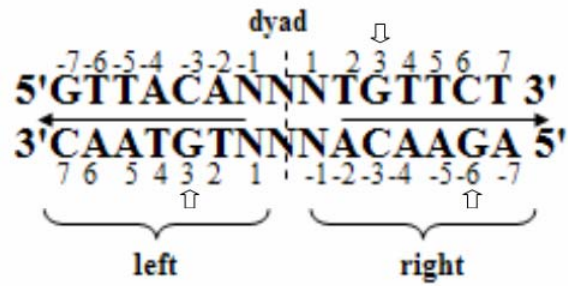


Figure 3.1 MMTV I GRE. The numbering convention employed here to refer to individual bases uses the dyad as origin, as indicated. The hexameric half-sites are indicated by arrows. G residues at which methylation prevents receptor binding are denoted by open arrows (Scheidereit and Beato, 1984).

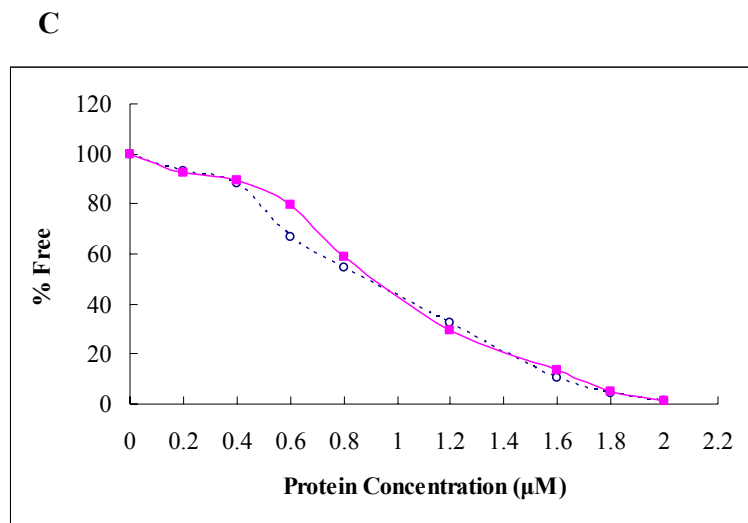
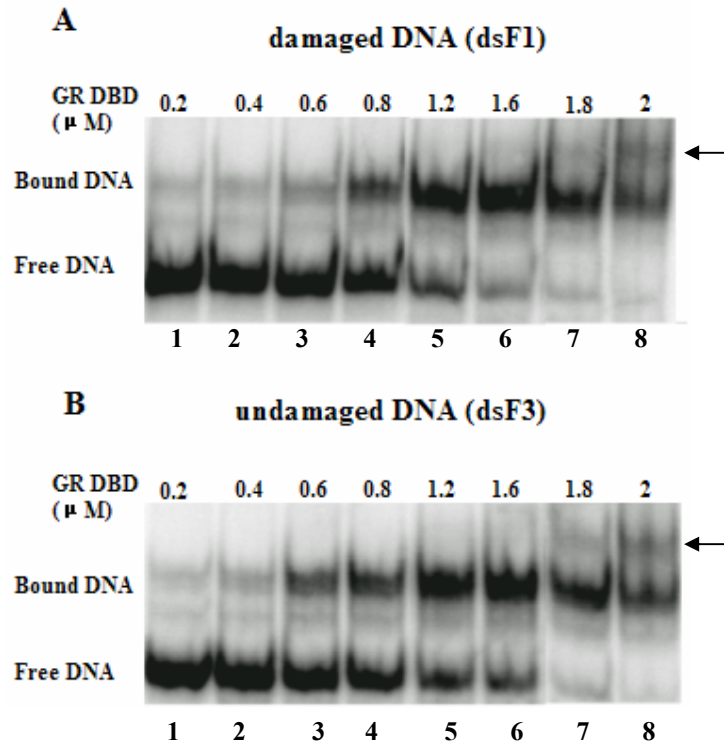


Figure 3.2 Comparison of GR DBD Binding to Damaged and Undamaged DNA. (A) GR DBD-damaged DNA (F1) complex. Binding reactions were performed with ~5 nM of labeled F1 DNA and increasing amounts of GR DBD. Bound and free DNA were separated on native polyacrylamide gels and quantified as described in Materials and Methods. (B) GR DBD-undamaged DNA (F3) complex. Binding reactions were performed with F3 DNA as described in panel A. (C) Plot of the percentage of free DNA as a function of protein concentration in damaged (solid line, ■) and undamaged (dashed line, ○) DNA. Arrows indicate the position of GR DBD dimer-GRE complexes.

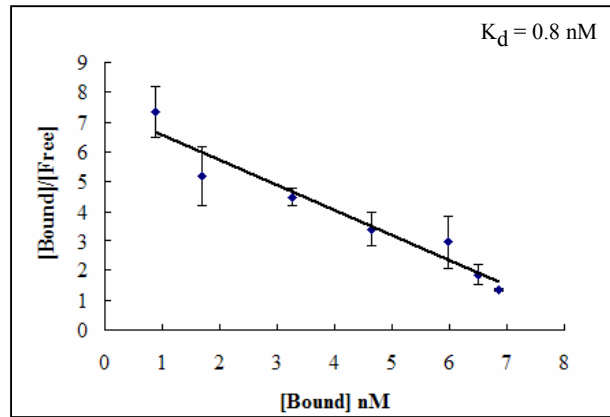
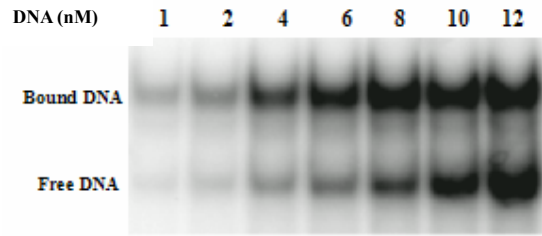
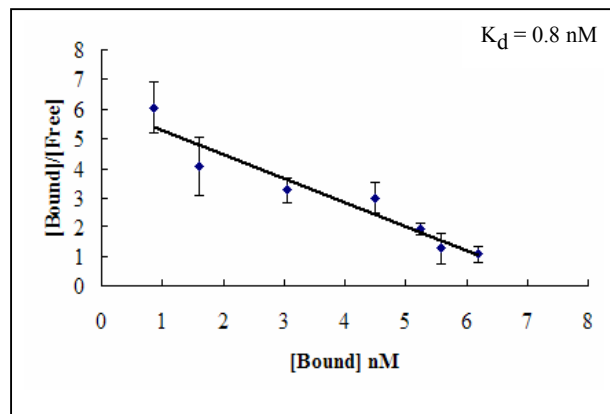
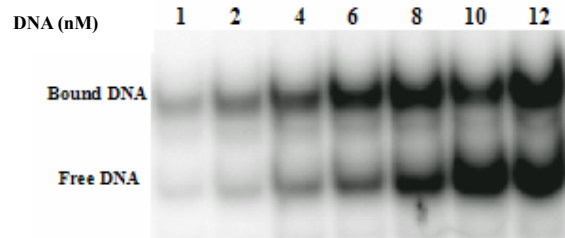
A**damaged DNA (dsF1)****B****undamaged DNA (dsF3)**

Figure 3.3 Determination of Apparent K_d Values of the GR DBD-DNA

Complexes. Panels show EMSA (upper panels) and Scatchard analysis (lower panels) of GR DBD-damaged DNA complex (A) and GR DBD-undamaged DNA complex (B). The ratio of [bound DNA] to [free DNA] was determined from gel scans and plotted *versus* [bound DNA]. Due to cooperative DNA binding of GR DBD, the Scatchard plots for intact and damaged DNA were nonlinear at low DNA concentrations (data not shown), and consequently, these points were excluded from the analysis. The K_d values were calculated from the slopes (m) of the linear regression fits of the data ($K_d = -1/m$). Each data point represents the mean ± 1 SD of three independent experiments.

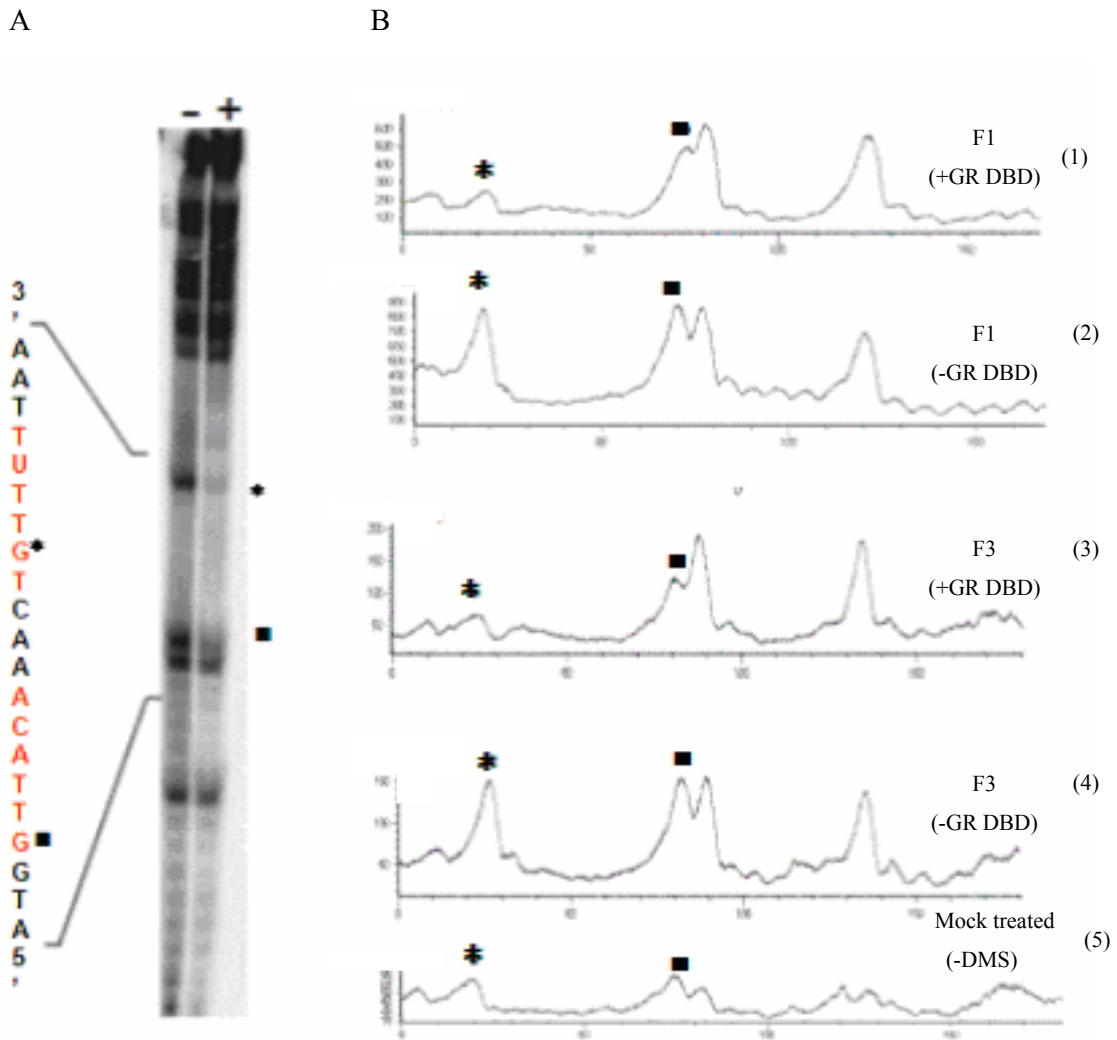
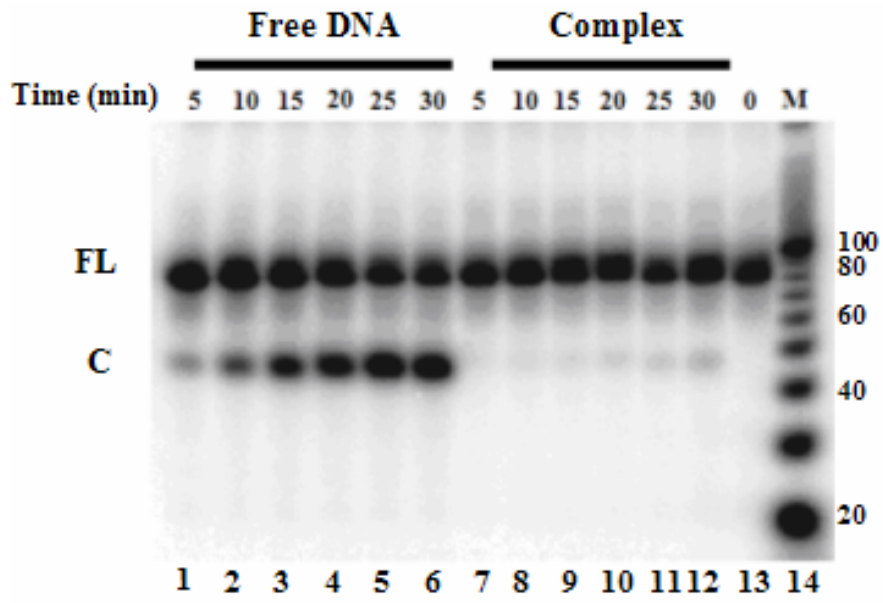
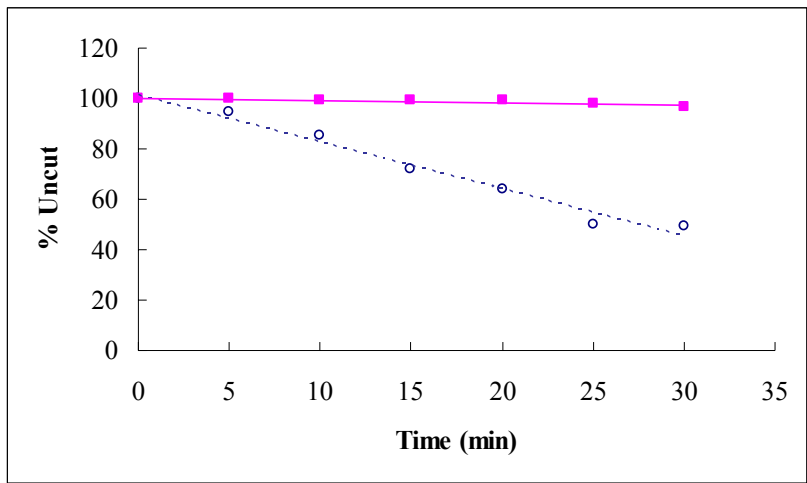


Figure 3.4 Methylation Protection of DNA Substrates by GR DBD. (A) Representative gel showing methylation of the damaged DNA substrate (dsF1) by DMS in the presence (+) or absence (-) of GR DBD. DNA was isolated as described in Materials and Methods, cleaved with 10% piperidine, and fractionated by denaturing gel electrophoresis. *, position of G in the right half-site of GRE. ■, position of G in the left half-site of GRE. (B) Gel scans for methylation of guanines in both the damaged (dsF1) and undamaged (dsF3) DNA substrates. (1) GR DBD-bound dsF1; (2) free dsF1; (3) GR DBD-bound dsF3; (4) free dsF3; (5) mock-treated dsF3 (-DMS).

A



B



C

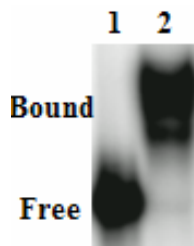
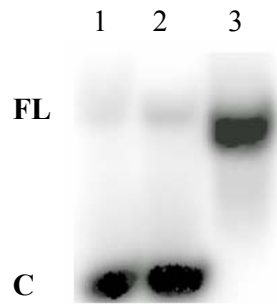
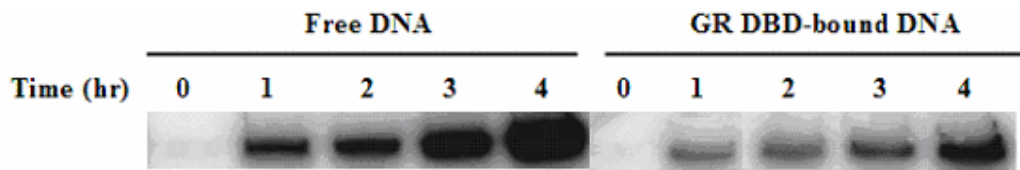


Figure 3.5 UDG and APE Digestions of Free and GR DBD-bound DNA. (A) Denaturing gels of free and GR DBD-bound DNA after incubation with UDG and APE. UDG/APE digestions were carried out for increasing times (5-30 min). The full-length bands (FL) indicate DNA resistant to UDG/APE digestions. The cleaved bands (C) indicate DNA fragments resulting from UDG/APE cleavage. Lane 13 shows the mock-treated DNA. M represents marker. (B) The percentage of intact DNA was plotted *versus* the incubation time for free DNA (dashed line, ○) and GR DBD-bound DNA (solid line, ■). (C) It was shown that all DNA in the GR DBD-containing set of experiments are in GR DBD-DNA complexes.

A



B



C

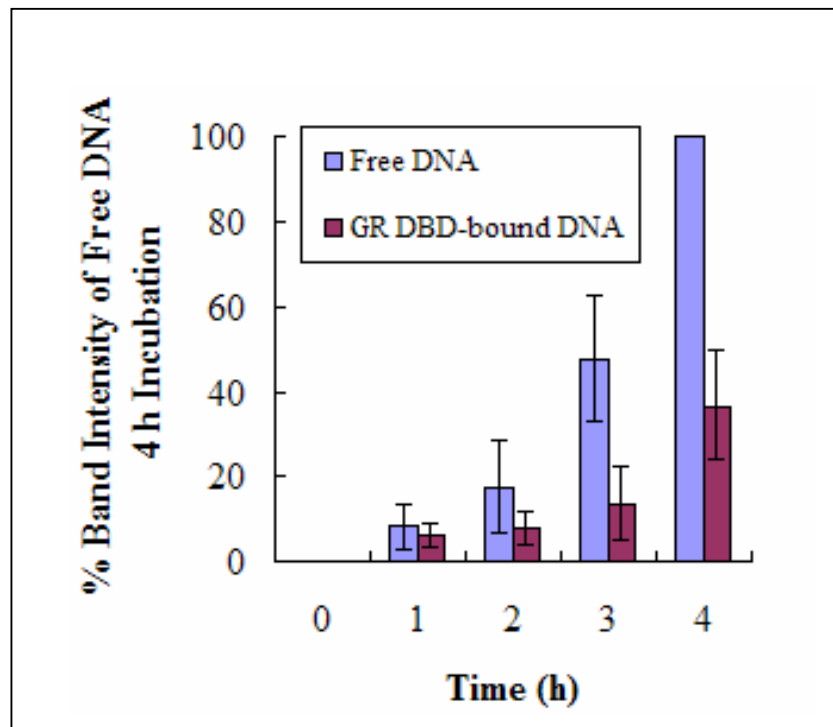


Figure 3.6 Synthesis by DNA Polymerase β on Free and GR DBD-bound DNA. (A) Denaturing gel showing UDG/APE digestion of free and GR DBD-bound DNA for 1.5 h. The full-length bands (FL) indicate DNA resistant to UDG/APE digestions. The cleaved bands (C) indicate DNA fragments resulting from UDG/APE cleavage. Lane numbers are denoted as follows: 1: free DNA digested by UDG/APE; 2: GR DBD-bound DNA digested by UDG/APE; 3: intact free DNA. (B) Denaturing gels of free and GR DBD-bound DNA showing the 5' end-labeled cleavage product and subsequent addition of radionucleotides to the 3' terminus. Incubation times are from 0 to 4 h with UDG, APE, and pol β . (C) Quantitative analysis of pol β synthesis. The ratio of each band intensity to the band intensity representing incorporation of [α - 32 P]dCTP in the free DNA after 4 h incubation was calculated and plotted *versus* the incubation time. Values represent the mean \pm 1 SD of three independent experiments.

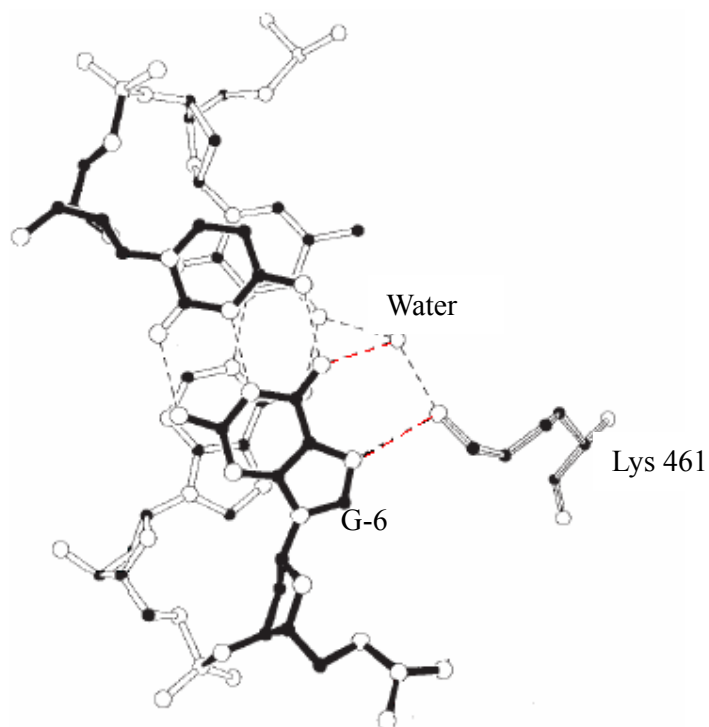


Figure 3.7 Hydrogen Bonds between G (-6) and Lys 461. G (-6) accepts one direct and one water-mediated hydrogen bonds from an invariant Lys 461 [adapted from (Luisi et al., 1991)]. Hydrogen bonds are indicated in red.

REFERENCES

- Beard, B.C. (2003) Thesis entitled "Base Excision Repair of Dynamic Chromatin Substrates".
- Beard, B.C., Wilson, S.H., and Smerdon, M.J. (2003) *Proc Natl Acad Sci U S A.* Jun 24; 100(13), 7465-7470.
- Bennett, R.A., Wilson, D.M., Wong, D., and Demple, B. (1997) *Proc Natl Acad Sci U S A.* Jul 8; 94(14), 7166-7169.
- Chen, H. and Shaw, B.R. (1993) *Biochemistry* 32 (14), 3535-3539.
- Clemens, K.R., Zhang, P., Liao, X., McBryant, S.J., Wright, P.E., and Gottesfeld, J.M. (1994) *J. Mol. Biol.* 244, 23-25.
- Dahlman, K., Strömstedt, P.-E., Rae, C., Jörnvall, H., Flock, J.-I., Carlstedt-Duke, J., and Gustafsson, J.-Å. (1989) *J. Biol. Chem.* 264, 804-809.
- Dahlman-Wright, K., Wright, A.P.H., and Gustafsson, J.-Å. (1992) *Biochemistry* 31, 9040-9044.
- Doetsch, P.W. (2002) *Mutation Research* 510, 131-140.
- Freeman, L.P., Luisi, B.F., Korszun, Z.R., Basavappa, R., Sigler, P.B., and Yamamoto, K.R. (1988) *Nature* 334, 543-546.
- Green, S. and Chambon, P. (1987) *Nature* 325, 75-78.
- Ham, J., et al. (1988) *Nucleic Acids Res.* 16, 5263-5267.
- Klock, G., Strähle, U., and Schütz, G. (1987) *Nature* Oct; 329 (22), 734-736.
- Lindahl, T. (1979) *Prog. Nucleic Acid Res. Molec. Biol.* 22, 135-192.
- Luisi, B.F., Xu, W.X., Otwinowski, Z., Freedman, L.P., Yamamoto, K.R., and Sigler, P.B. (1991) *Nature* 352, 497-505.
- Necela, B.M. and Cidlowski, J.A. (2004) *J Biol Chem.* Sep 17; 279(38), 39279-39288.
- Nelson, C.C., Hendy, S.C., Shukin, R.J., Cheng, H., Bruchofsky, N., Koop, B.F., and Rennie, P.S. (1999) *Mol. Endocrinol.* 13, 2090-2107.

- Nilsen, H., Lindahl, T. and Verreault, A. (2002) *EMBO J.* 21(21), 5943-5952.
- Nordeen, S.K., Suh, B.J., Kuhnel, B., and Hutchison, C.A., (1990) *Mol. Endocrinol.* 4, 1866-1873.
- Olsen, L.C., Aasland, R., Wittwer, C.U., Krokan, H.E., and Helland, D.E. (1989) *EMBO J.* Oct; 8(10), 3121-3125.
- Parikh, S.S., Mol, C.D., Slupphaug, G., Bharati, S., Krokan, H.E., and Tainer, J.A. (1998) *EMBO J.* Sep 1; 17(17), 5214-5226.
- Rousseau, G.G. (1984) *Molecular and Cellular Endocrinology* 38, 1-11.
- Sancar, A., Lindsey-Boltz, L.A., Unsal-Kacmaz, K., and Linn, S. (2004) *Annu Rev Biochem.* 73, 39-85.
- Stivers, J.T., Pankiewicz, K.W., and Watanabe, K.A. (1999) *Biochemistry* Jan 19; 38(3), 952-63.
- Strauss, P.R., Beard, W.A., Patterson, T.A., and Wilson, S.H. (1997) *J Biol Chem.* Jan 10; 272(2), 1302-1307.
- Tsai, S.Y., Carlstedt-Duke, J., Weigel, N.L., Dahlman, K., Gustafsson, J., Tsai, M., and O'Malley, B.W. (1988) *Cell* 55, 361-369.
- Scheidereit, C. and Beato, M. (1984) *Proc. Natl. Acad. Sci. USA.* 81, 3029-3033.
- Srivastava, D.K., Vande Berg, B.J., Prasad, R., Molina, J.T., Beard, W.A., Tomkinson, A.E., and Wilson, S.H. (1998) *J. Biol. Chem.* Aug 14; 273(33), 21203-21209.
- Verri, A., Mazzarello, P., Biamonti, G., Spadari, S., and Focher, F. (1990) *Nucleic Acids Res.* Oct 11; 18(19), 5775-5780.
- Wink, D.A., Kasprzak, K.S., Maragos, C.M., Elespuru, R.K., Misra, M., Dunams, T.M., Cebula, T.A., Koch, W.H., Andrews, A.W., Allen, J.S., and Keefer, L.K. (1991) *Science* 254, 1001-1003.